AD-A088 362 TRW DEFENSE AND SPACE SYSTEMS GROUP REDONDO BEACH CA F/G 22/1
NUCLEAR HARDNESS EVALUATION PROCEDURES FOR THE PRELIMINARY ASSE--ETC(U)
DEC 79 D M CLEMENT, A R CARLSON, W H ROWAN DNA001-78-C-0306
UNCLASSIFIED DNA-5114F NL

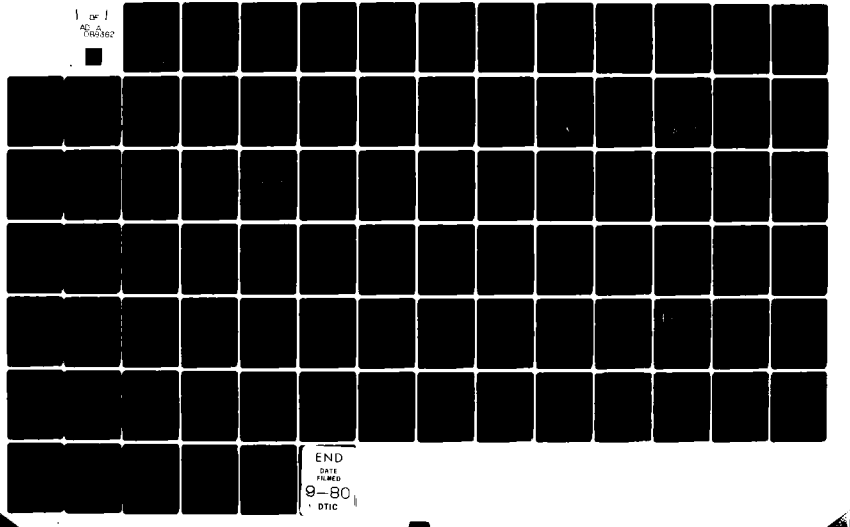

(10) LEVEL II

DNA 5114F

NUCLEAR HARDNESS EVALUATION PROCEDURES FOR THE PRELIMINARY ASSESSMENT OF THE FLEETSATCOM ATTITUDE AND VELOCITY CONTROL SUBSYSTEM

TRW Defense and Space Systems Group
One Space Park
Redondo Beach, California 90278

1 December 1979

Final Report for Period 1 January 1979—1 December 1979

CONTRACT No. DNA 001-78-C-0306

APPROVED FOR PUBLIC RELEASE;
DISTRIBUTION UNLIMITED.

THIS WORK SPONSORED BY THE DEFENSE NUCLEAR AGENCY
UNDER RDT&E RMSS CODE B323079464 R99QAXEE50328 H2590D.

Prepared for
Director
DEFENSE NUCLEAR AGENCY
Washington, D. C. 20305

Destroy this report when it is no longer needed. Do not return to sender.

PLEASE NOTIFY THE DEFENSE NUCLEAR AGENCY, ATTN: STTI, WASHINGTON, D.C. 20305, IF YOUR ADDRESS IS INCORRECT, IF YOU WISH TO BE DELETED FROM THE DISTRIBUTION LIST, OR IF THE ADDRESSEE IS NO LONGER EMPLOYED BY YOUR ORGANIZATION.

DNA PRINTING PLANT

(18) DNA, SBIE

UNCLASSIFIED

SECURITY CLASSIFICATION OF THIS PAGE (When Data Entered)

(19) **REPORT DOCUMENTATION PAGE**

READ INSTRUCTIONS BEFORE COMPLETING FORM

1. REPORT NUMBER: DNA 5114F, AD-E300 878	2. GOVT ACCESSION NO.: AD-A088362
3. RECIPIENT'S CATALOG NUMBER	
4. TITLE (and Subtitle): NUCLEAR HARDNESS EVALUATION PROCEDURES FOR THE PRELIMINARY ASSESSMENT OF THE FLEETSATCOM ATTITUDE AND VELOCITY CONTROL SUBSYSTEM.	5. TYPE OF REPORT & PERIOD COVERED: Final Report for Period 1 Jan 79 — 1 Dec 79
	6. PERFORMING ORG. REPORT NUMBER
7. AUTHOR(S): D. M. Clement, A. R. Carlson, W. H. Rowan	8. CONTRACT OR GRANT NUMBER(s): DNA 001-78-C-0306
9. PERFORMING ORGANIZATION NAME AND ADDRESS: TRW Defense and Space Systems Group, One Space Park, Redondo Beach, California 90278	10. PROGRAM ELEMENT, PROJECT, TASK AREA & WORK UNIT NUMBERS: Subtask R99QAXE503-28
11. CONTROLLING OFFICE NAME AND ADDRESS: Director, Defense Nuclear Agency, Washington, D.C. 20305	12. REPORT DATE: 1 December 1979 (11) (19) E503; 13. NUMBER OF PAGES: 82
14. MONITORING AGENCY NAME & ADDRESS (if different from Controlling Office) (12) 87	15. SECURITY CLASS (of this report): UNCLASSIFIED
	15a. DECLASSIFICATION DOWNGRADING SCHEDULE

16. DISTRIBUTION STATEMENT (of this Report)

Approved for public release; distribution unlimited.

17. DISTRIBUTION STATEMENT (of the abstract entered in Block 20, if different from Report)

18. SUPPLEMENTARY NOTES

This work sponsored by the Defense Nuclear Agency under RDT&E RMSS Code B323079464 R99QAXEE50328 H2590D.

19. KEY WORDS (Continue on reverse side if necessary and identify by block number)

Nuclear Weapon Effects	SGEMP
X-rays	TREE
Nuclear Hardness Evaluation Procedures	Functional Upset
NHEP	Thermomechanical
Satellites	

20. ABSTRACT (Continue on reverse side if necessary and identify by block number)

This document summarizes the procedures to be followed for the preliminary assessment of the attitude and velocity control subsystem of the FLSATCOM satellite to various nuclear weapon effects.

DD FORM 1 JAN 73 1473 EDITION OF 1 NOV 65 IS OBSOLETE

UNCLASSIFIED

SECURITY CLASSIFICATION OF THIS PAGE (When Data Entered)

409657

TABLE OF CONTENTS

LIST OF ILLUSTRATIONS

LIST OF ILLUSTRATIONS (Continued)

LIST OF TABLES

SECTION 1

INTRODUCTION

1.1 ASSESSMENT OBJECTIVES AND SCOPE.

This document presents assessment procedures for the preliminary assessment of the survivability of the FLTSATCOM satellite Attitude and Velocity Control Subsystem (AVCS) to various nuclear weapon effects (NWE). In addition to obtaining the assessment results themselves the objectives of this assessment are primarily to exercise for the first time the NHEP (Nuclear Hardness Evaluation Procedures) assessment methodology for satellites on a real piece of satellite equipment and to identify technology and/or data gaps that hinder the assessment. The AVCS was selected first for consideration because it is rather compact (one major box of electronics and assorted sensors) and at the same time it is representative of satellite electronics on FLTSATCOM. Other FLTSATCOM subsystems will be considered later.

The term "preliminary assessment" has a rather specialized meaning in the context of the NHEP methodology. This methodology is reviewed in Section 1.2 in more detail, but we would like to indicate the major characteristics of a preliminary assessment as described here, namely, it performs a quantitative assessment of the vulnerability of mission critical equipment of a satellite to various NWE using existing data as well as simple algorithms in order to identify the controlling failure modes of the system. Later phases of the NHEP methodology may develop new data via test or analyses, but this preliminary assessment is based on existing data only. Most of the data identified here were obtained from two basic sources of information, both of which were documented during the FLTSATCOM hardened satellite development program. These documents are:

- FLTSATCOM Survivability Critical Design Review Package, 15 July 1974[1)]
- Spacecraft Hardening Design Guidelines Handbook[2)]

The former document (referred to henceforth as the CDR package) summarizes the hardness data obtained by TRW's Vulnerability and Hardness Laboratory (V&H) in the course of the FLTSATCOM program. The latter document (referred to as the Guidelines) distills the V&H Lab's experience in contributing to the design of hardened satellite systems. The adequacy of the data, for the purposes of a preliminary assessment, is discussed in Section 1.3.

The specific NWE to which the AVCS is assessed are the following:

- SGEMP burnout
- TREE burnout (photo-current)
- permanent degradation from total dose (n, γ and fission electrons)
- functional upset (all NWE)
- radiation effects on nonelectronic components

The NWE to which the AVCS is <u>not</u> assessed are the following:

- EMP burnout
- synergistic effects (TREE + SGEMP)
- Short term displacement damage

EMP burnout is not treated partly because it is not considered a threat to satellites in geosynchronous orbits, but more importantly because we are unsure how to relate EMP environments at geosynchronous altitudes to weapon parameters and height of burst. These parameters are important if one wants to make comparisons of EMP to different NWE originating from the same weapon(s). The last two effects mentioned above are not considered simply because no data was acquired for them in the original FLTSATCOM program. Later phases of the assessment beyond the preliminary assessment would in principle address the NWE omitted in the preliminary assessment.

Both the assessment procedures and the assessment itself which will eventually follow are a joint effort of TRW and ETI. This assessment plan represents the bringing together of the following sources of information which are described in more detail in the sections which follow.

1) NHEP methodology and flow charts (developed by ETI): Section 1.2

2) top level screen of the AVCS (performed by ETI): Section 1.4

3) statistical management of data and assessment (developed by TRW): Section 2

4) specific procedures for detailed assessment (developed by TRW): Section 3

The NHEP methodology itself is represented in a set of general flowcharts which were followed closely in setting up the present assessment procedures, taking into account the specific hardening features of FLTSATCOM. The top level screen, performed sometime ago by ETI,[3] succeeded in isolating the subsystems and boxes of FLTSATCOM that were both susceptible to various NWE as well as critical to on-orbit functions. It should be pointed out that some 10,000 failure modes exist on the AVCS subsystem alone,

and that careful management of the data using statistical tools is a critical part of the assessment plan. By specific procedures we mean the detailed formulas, graphs, and algorithms to be followed in the assessment of each failure mode.

The organization of the assessment is discussed in Section 1.5.

The specific procedures of the assessment for each NWE are discussed in Section 3.

1.2 OVERVIEW OF THE NHEP METHODOLOGY.

Before presenting the details of our assessment plan we would like to discuss some topics related to the background of NHEP-S in order to place our present efforts into an understandable context. The topics to be discussed here are as follows:

- what is NHEP and its overall objective relative to a satellite assessment methodology?
- who would use NHEP?
- what does the NHEP methodology look like?
- what progress has been made in developing NHEP?

What is NHEP?

NHEP is a methodology which produces in principle a complete assessment of a system to all nuclear weapon effects. It was originally developed by Effects Technology Incorporated (ETI) and applied to the problem of assessing re-entry vehicles.

Can NHEP be applied to satellites?

While the NHEP re-entry vehicle program was successful, it should be pointed out that it was not at all clear that the methodology could be applied to satellites for the following reasons: 1) the vulnerability of electronics had not been assessed in the earlier program, and 2) the number of potential failure modes in a satellite system is at least an order-of-magnitude larger than for re-entry vehicles. For these reasons our present efforts have been devoted to determining the feasibility of applying NHEP to satellites. By feasibility we mean the following:

- one should be able to write down a complete methodology for evaluating satellite hardness;
- there should be no insurmountable technology or data gaps, i.e. with some reasonable amount of funding, or perhaps with a revision of the methodology, one can foresee obtaining sufficient data to exercise NHEP;

- the methodology should be demonstrated on a real piece of satellite equipment, e.g. a subsystem of a satellite.

What is the output of NHEP?

The output of NHEP consists of the following. First and foremost NHEP produces damage functions which represent the satellite's probability of survival P_S as a function of environment, as shown in Figure 1.2-1, where the distribution of P_S depends on both random and bias uncertainties associated with the input data. By arraying where possible damage functions for each nuclear weapon environment on the same graph, the virtues of NHEP become readily apparent, namely,

- NHEP allows management control of resources in either a satellite hardening program or an assessment effort or both by concentrating effort on the controlling failure modes;
- NHEP determines not only the degree of survivability at a specified criteria environment, but also the environment (stress level) at which the satellite fails for nuclear weapon effect;
- NHEP identifies gaps in the technology base.

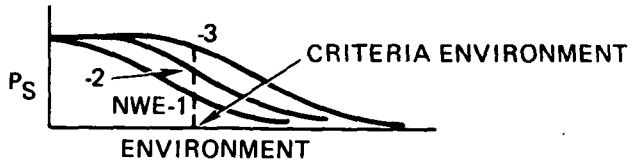

Figure 1.2-1. NHEP-S Damage Functions

Who would use NHEP?

We envision that NHEP-S could be used by the following organizations:

- Planners, who for example are interested in satellite survivability as a function of threat scenarios
- Procurement groups, who want to know if it is feasible to design hardened satellites and the associated costs
- technology development groups, who might want to identify technology needs, as well as prioritize them
- satellite program planners, who want to allocate hardness resources in a satellite program.

From the point of view of a system house, NHEP-S (provided it were tied into system level requirements in a satellite program) would have an impact because it would enable program planners to allocate hardening resources among different nuclear

weapon effects. Managers could decide, for example, whether further hardening was required in the course of a program, or what kinds of additional data in the form of tests or improved analysis were required. This contrasts with the present situation where hardness to each nuclear weapon effect is treated independently, regardless of its relative importance to the satellite's overall hardness.

In developing NHEP-S, we have consciously attempted to make it an integral tool in a satellite hardening program. We do not mean to imply, however, that the methodology could not be applied as a straight assessment tool (i.e., after the system is built), nor that it could not be applied to an unhardened system.

Overview of NHEP Methodology.

An overview of NHEP is shown in Figure 1.2-2. Basically there is a five step procedure with an inner DO loop on the last three steps indicating subphases of the assessment. These subphases are called "preliminary assessment," "data base improvement," and "final assessment."

Step 1: Determination of the management acceptance criteria. Here the manager decides, for example, the minimum probability of survival he will accept at a criteria environment or he may assign screening criteria for circuits based on the concept of a failure budget, i.e., the failure rate for circuits for SGEMP burnout is only 2% at a criteria environment. (Of course, the manager may also choose not to impose any criteria on the assessment.)

Step 2: Top level screen or "logic" screen where the system is screened based on the criticality of circuits and whether they are used to perform on-orbit functions.

Step 3: The assignment by the manager of assessment and/or hardening resources for each phase of the assessment.

Step 4: Carrying out the assessment procedures for each phase.

Step 5: Screening of circuits after each assessment phase in order to concentrate on the controlling circuit failure modes.

Note that the subphases of the assessment imply carrying out procedures of increasing complexity. Whereas step 2 (called "Top Level Screen") is a logic screen (i.e., no detailed data, formulas, etc.) the assessment subphase called "preliminary assessment" involves the use of existing data along with simple algorithms. These results are used to screen the circuits, thus concentrating attention in the later assessment phases on the controlling failure modes. The last two phases of assessment involve various levels of hardening options, development testing, model improvement, and finally system/subsystem level validation testing.

NHEP-S PROCEDURE OVERVIEW

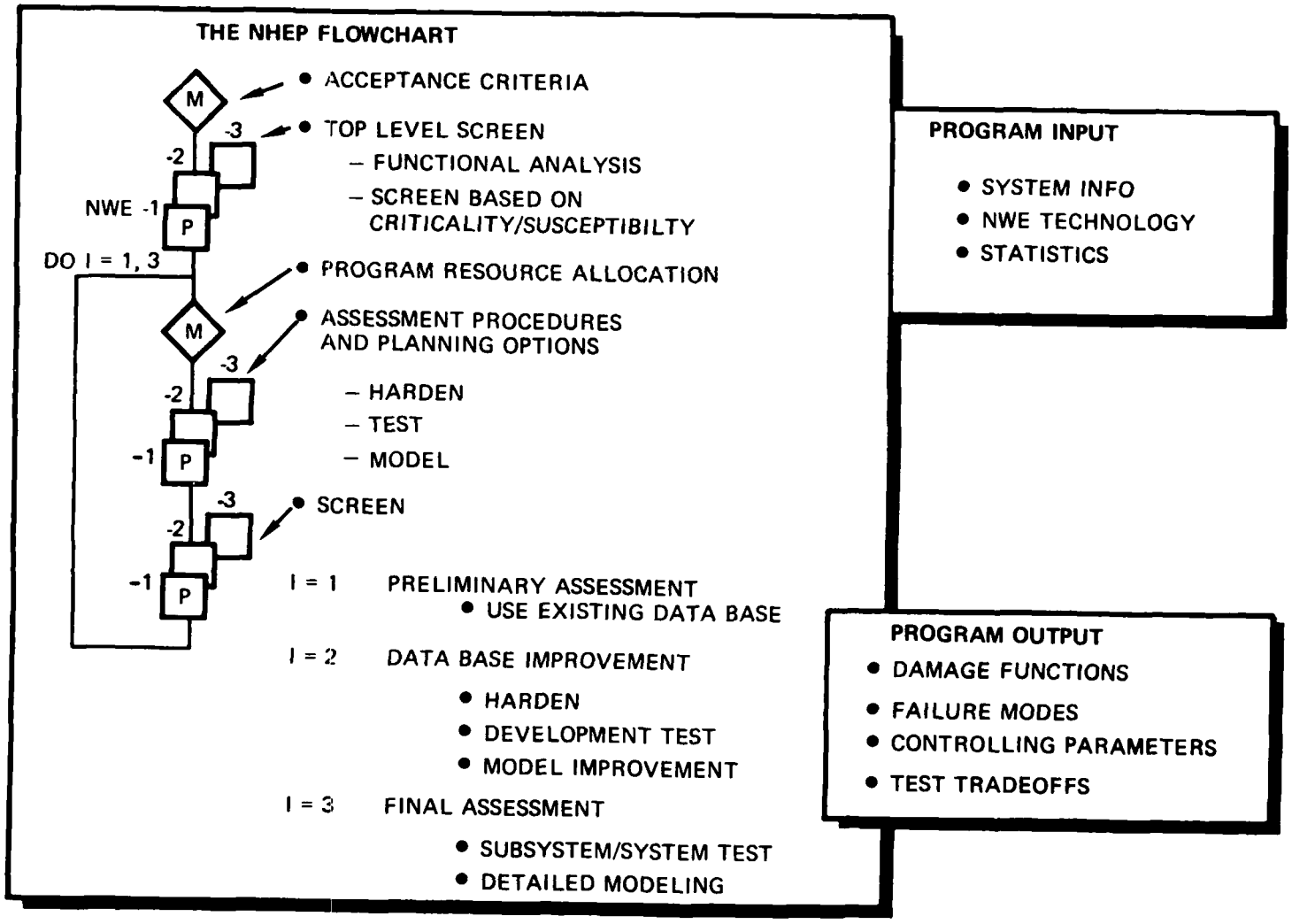

Figure 1.2-2. NHEP-S Procedure Overview

What progress has been made?

For the past year TRW and ETI have been developing the NHEP methodology whose overall objective is to form the basis of an assessment of a satellite system to all nuclear weapon effects. The immediate objective of our present efforts has been:

1) to see if it is possible to write down an appropriate methodology;

2) to see if there are any insurmountable technology gaps which would prevent the application of the methodology;

3) to demonstrate the methodology by application to a satellite subsystem.

Progress in reaching these goals (November 1979) is as follows:

1) flowcharts for all of the various nuclear weapons effects have been written (ETI);

2) specific procedures have been developed by TRW for the treatment of SGEMP and TREE burnout, permanent degradation, and an approach to the assessment of functional upset has been outlined; ETI has written specific procedures for radiation effects on nonelectronic components including thermomechanical damage and material degradation. These procedures are presented in Section 3.

3) the so-called top-level screen of the AVCS assessment which ETI performed some time ago is reviewed in Section 1.4.

1.3 OVERVIEW OF FLTSATCOM SURVIVABILITY DATA.

By definition the preliminary assessment of a satellite relies on the existing data base. In this case the existing survivability data was collected in the course of the development and qualification test program for FLTSATCOM. However, it cannot be overemphasized that this data was not collected to support an assessment effort. Rather it was collected to support the specific customer imposed requirements related to survivability. The corrolary is that the existing data, for our purposes at least, is often incomplete and/or not in the most desirable form.

We are not daunted by this. In fact the identification of missing data in the FLTSATCOM data base may cause a re-evaluation of the kinds of data actually collected in future hardened satellite programs. For our present purposes, however, we want to emphasize that the survivability data was tailored both to the specific hardening decisions made in the FLTSATCOM program as well as the customer imposed requirements. For this reason it is appropriate here to discuss

- the survivability requirements on FLTSATCOM
- the available data for each of the NWE

There are two points to keep in mind about the FLTSATCOM hardening effort. First, FLTSATCOM was designed to meet a set of specified criteria environments, i.e., hardness to so much X-ray, γ, neutron flux, as well as total dose. The verification requirements were that individual parts or components be tested at anywhere from 1 to 10 times the specified criteria environment. From the point of view of NHEP this represents a rather severe impact since NHEP is concerned not only with criteria environments, but also much higher environment levels. In other words, at what threat level does a satellite break? For this reason, the FLTSATCOM data is often incomplete for the purposes of the NHEP assessment.

The second point is that the development and verification tests done on FLTSATCOM were concentrated mostly at the piece-part level (n, γ, FXR) with some subsystem level upset testing using the FXR (Vulcan). This situation is partly due to the fact that the technology for system level tests (in the form of suitable simulators and acceptable procedures) was not available at the time of the RFP and the customer was unwilling to impose unrealizable requirements. For example, the SGEMP burnout hardness verification was required to be performed by analysis only, and the scheduled system level EMP test was cancelled because the threat environment was later judged to be too small to affect the electronics. It is expected that in the future, as the technology progresses, the appropriate system or subsystem level tests will become a standard feature of the hardening programs.

Again, the lack of system or subsystem level test data places constraints on the assessment. For example we assume in most cases that a part fails (burns out) or degrades independent of every other part. If one assumes this is true, and proceeds to design a test program based on lot sample testing of parts, it is difficult to see how an assessment program based on available data can verify this assumption.

Two final difficulties associated with lot sample testing: On FLTSATCOM every single lot of parts (300-400 lots) had 5 parts sampled at some overstress level relative to a criteria environment. It is our assertion that the amount of limited testing done is insufficient of itself to provide statistical confidence in hardness. It should be pointed out, however, that the lot sample testing was a customer imposed requirement in order to establish a more-or-less uniform standard of acceptability on the part suppliers.

This brings up the issue of process variability and process changes leading to different radiation vulnerability for the same generic part, sometimes even from the same manufacturer. It was found that such process sensitivity resulted in changes of response of up to an order-of-magnitude between the design baseline data developed on

the basis of the engineering tests and the data exhibited by lot sample tests on production parts. Such changes occasionally required design "fixes" (e.g. adding shielding) to compensate for the differences in radiation response. This will require us in our assessment effort to run down these design changes, which were installed after the CDR package was written.

The kinds of data available on FLTSATCOM for the NWE considered in this assessment are summarized in Table 1.3-1. Comments on the data are indicated there. More detailed comments are reserved for Section 3 where the various NWE are discussed in detail.

1.4 ASSESSMENT CRITERIA AND TOP LEVEL SCREEN FOR FLTSATCOM.

The steps in the NHEP-S methodology, up to and including the preliminary assessment phase in Figure 1.2-2, are

1. set acceptance criteria
2. perform top level screen
3. allocate program resources
4. perform preliminary assessment and planning options
5. screen

We discuss the first two here.

Acceptance Criteria.

There are a number of requirements that a manager can impose on an assessment. These might, for example, be concerned with required accuracy of the calculations. Perhaps the manager wants to obtain a required probability of survival at a criterion environment. Or, perhaps no assessment acceptance criteria are imposed.

For the present we have not imposed any acceptance criteria on the preliminary assessment since we want to see all the implications of the methodology before narrowing ourselves down. One task which we will define for ourselves is to investigate the consequences of various acceptance criteria on subsequent phases of the assessment.

Top Level Screen

Referring to Figure 1.2-2 which gives the overview of the NHEP-S methodology the second major step in the methodology is the top level screen which, without the benefit of actual calculations, surveys the satellite and identifies

Table 1.3-1. Test Data Available for Assessment of AVCS

NWE	Data Source	Data	Adequacy of Data for Assessment
SGEMP Burnout	• CDR package, Ref 1	• cable source terms for direct injection	• adequate
	• Refs 4,5	• cable source terms for direct injection	
	• CDR package, Ref 1	• shielding effectiveness of cables	• data is not sufficient for obtaining cable transfer functions or verifying that direct injection dominates
	• CDR package, Ref 1	• Wunsch-Bell damage constants	• based on Ref. 6 for generic parts only
	• Boeing/AFWL data, Ref 6	• Wunsch-Bell damage constants	• FLTSATCOM specific parts not included
	• CDR package, Ref 1	• effectiveness of terminal protection	• single shot tests of terminal protection on engineering model circuits
		• current injection tests on system or circuits	• no data
TREE Burnout	• CDR package, Ref 1	• lot sample tests, 5 parts/lot, 300-400 lots at 10X criteria using Vulcan FXR	• no test-to-failure data, no statistical confidence in hardness
Degradation (n, γ, e)	• CDR package, Ref 1	• lot sample tests, 5 parts/lot, 300-400 lots at 2X and 10X criteria for n and Co^{60} combined, observed long term parameter degradation (deratings)	• no separate breakout of n and γ deratings • derated parameter values used as the design standard
Functional Upset	• Flash X-ray test report, Ref 7	• six tests on AVCS at criteria environment, TRW Vulcan FXR	• test designed to verify fault tolerant design, but limited data implies limited statistical confidence
Radiation effects on nonelectronic components	• CDR package, Ref 1, Design Guidelines, Ref 2	• no test data generated	

- what components of the satellite are vulnerable to particular NWE
- what components are used to perform on-orbit functions, i.e., what components are mission critical

If the given component is not used on orbit or is invulnerable to a given NWE, or both, it is discarded.

The virtues of the top level screen are as follows: besides getting rid of components, the top level screen

- organizes the way in which the satellite is viewed for potential damage to a given NWE
- establishes an audit trail in the form of a response/susceptibility matrix

Concerning the first point the failure modes for the various NWE considered in this assessment are:

NWE	Failure Mode
SGEMP burnout	circuit
TREE burnout	part
degradation	part
functional upset	subsystem functions
radiation effects on nonelectronic components	system

In other words, the failure mode for SGEMP burnout, for example, is the failure of an individual circuit, and in fact, these will be identified in the subsequent assessment by the box and pin number at the interface between incident cabling and interior box circuitry. In contrast, functional upset occurs at the subsystem level and is identified, not by the boxes and circuitry, but by the specific function.

The second point above, namely the response/susceptibility matrix, was generated by ETI for the entire FLTSATCOM system, i.e., the top-level screen of FLTSATCOM is complete. The results for the AVCS subsystem are shown in Table 1.4-1. Those AVCS boxes which can be eliminated from any further analysis and the justification are indicated. The blank spaces indicate those boxes that still have to be considered for the indicated NWE. A more extensive discussion of this top level screen is given in Ref. 3 by ETI.

Table 1.4-1. Response/Susceptibility Matrix for AVCS Boxes

SUBSYSTEM	BOX	RESPONSE MODES: TRANSIENT — IONIZATION UPSET (FUNCTION)	IEMP UPSET (FUNCTION)	SGEMP UPSET (FUNCTION)	S.T. DISPLACEMENT (PART)	DEMP UPSET (FUNCTION)	SPACECRAFT CHARGING (FUNCTION)	COMBINED DRIVERS	COMBINED ELEMENTS	IONIZATION BURNOUT (PART)	TOTAL DOSE (PART)	IEMP BURNOUT (PART)	SGEMP BURNOUT (PART)	L.T. DISPLACEMENT (CIRCUIT)	DEMP BURNOUT (CIRCUIT)	SPACECRAFT CHARGING (CIRCUIT)	THERMOMECHANICAL (SYSTEM)	COMBINED DRIVERS	COMBINED ELEMENTS	PRE	DURING	POST — FUNCTION PERFOR.
AVCS	SUN SENSOR ASSEMBLY	○	○	○	○	○	○	△	△													
AVCS	SPINNING EARTH SENSOR ASSEMBLY	□	□	□	□	□	□	△	△													
AVCS	EARTH SENSOR ASSEMBLY		▽	▽		▽	▽		△													
AVCS	EARTH SENSOR ELECTRONICS																					
AVCS	AUX ELECT/ CON. ELEC. ASSEMBLY																					
AVCS	REACTION WHEEL ASSEMBLY																					
AVCS	SOLAR ARRAY DRIVE ASSEMBLY																					
AVCS	NUTATION DRIVE ASSEMBLY	△	△	△	△	△	△	△	△	△		△	△	△	△	△		△	△			

For each NWE the appropriate failure mode designation is indicated by the following key

△ = not credible

▽ = not lead to mission failure

○ = not mission critical

□ = not used on orbit

blank = box has not been screened out

1.5 OVERVIEW OF THE PRELIMINARY ASSESSMENT.

The status of the preliminary assessment of the AVCS is as follows. The NHEP methodology has been translated into a set of procedures for each NWE which will be applied to the AVCS. The documents necessary for the assessment have been gathered together; the formats for collecting the data have been identified; the statistical approaches to handling the data have been laid out, and the modeling approaches have been developed.

Our tentative schedule for completing the assessment based on these procedures is late January 1980. At the moment, since an assessment of a satellite has never been performed before, we do not know if our schedule is optimistic or pessimistic. In any case, while the assessment results themselves will be undoubtedly interesting, one of our objectives is to debug the methodology, and if necessary we will halt the assessment to rectify deficiencies in the methodology.

For purposes of this assessment each of the NWE is treated independently. This means that each of the NWE can be assessed separately, i.e., by different individuals working independently. This makes the organization of the assessment easy, and in fact an actual assessment of a system would parcel out NWE among different departments or performing organizations.

What is different about NHEP-S is that the performers come back to the assessment manager with damage functions for each NWE. The damage functions then get compared, and resources get allocated based on the damage functions.

It is this interactive feature of NHEP that we wish to highlight, and this is shown in Figure 1.5-1. At the point where all the preliminary damage functions are reported to the manager, a set of planning options will be investigated. These options will be resolved by considering what might happen to the damage functions if each of them are exercised. The cost of exercising the option will also be considered. For example, once we see the damage function for SGEMP burnout, we may ask what is the consequence of using semi-rigid cabling, as opposed to the standard braid shield in the AVCS. (The answer is, the additional size and weight make this option unattractive, but the fact that the option is considered and documented is very useful to a program manager.) Other options considered would be additional tests and/or improving the models. The resulting tradeoffs will define what happens on the next phase of the assessment.

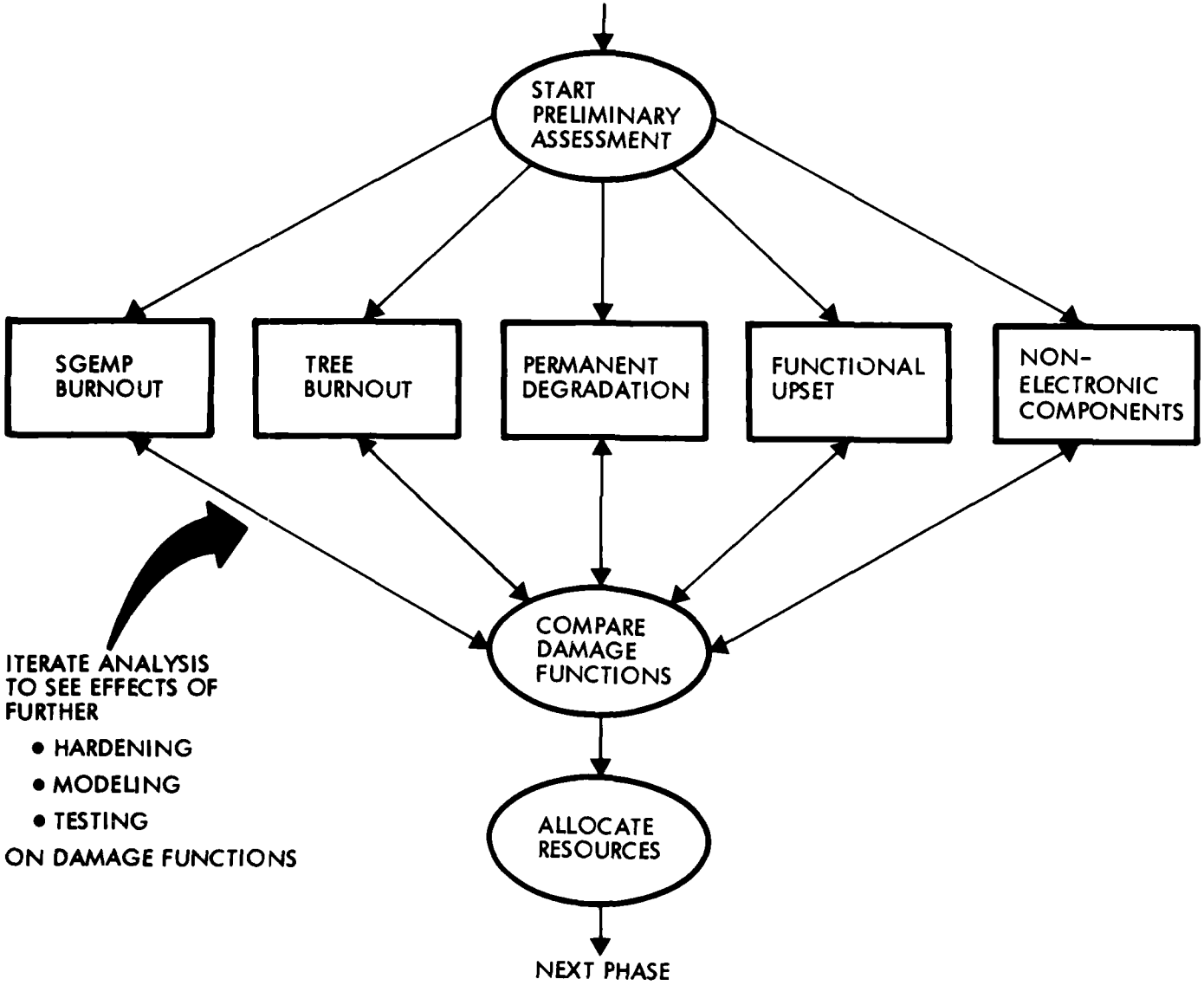

Figure 1.5-1. Plan for the Preliminary Assessment of the AVCS

SECTION 2

NHEP STATISTICAL APPROACH

2.1 OVERVIEW OF STATISTICAL MANAGEMENT OF PRELIMINARY ASSESSMENT.

Our objective in this section is to describe our approach to the statistical aspects of NHEP during the Preliminary Assessment phase. We assume in principle that prior to this phase certain boundary conditions have been defined. These include assessment accuracy acceptance criteria and identification of mission critical failure modes based upon a functional analysis. During the preliminary assessment phase the assessment is to be accomplished using only existing data and models. Naturally the accuracy of this first phase of the assessment may not satisfy the acceptance criteria. If this is the case then plans must be developed for improving the data and modeling base for the final assessment. The management function then enters to allocate resources to implement the plans during the next, Data Base Improvement, phase.

In this chapter we restrict our attention to the statistical aspects of the preliminary assessment phase. The following steps are involved: 1) development of the necessary failure mode inputs and models from existing data, 2) extraction of the necessary system data from drawings, 3) performance of required statistical calculations on the data base to generate statistical assessment results including damage functions. These show the distribution of resistance or strength of the satellite system and its component subsystems with measures of confidence in these results. And finally one considers how statistical decision-aiding information is generated such that management can use it to allocate resources during the next assessment phase, namely, data base improvement.

An overview of the assessment information flow during the preliminary screen phase is shown in Figure 2.1-1. We first discuss this figure in general terms, and then follow up with a specific statistical example in Section 2.2. Start with a typical failure mode depicted in the lower left of the figure. We will consider such failure modes in three parts, the cable and its lead to the pin, the subsequent protective circuitry, and the one or more devices such as transistors which are subject to failure. As shown in the center panel, we will define a certain number of classes for each of these. For example, one such device class may be the 2N2222 transistor. We will define a number of classes appropriate to the resolution of accuracy of the available data.

PRELIMINARY SCREEN ASSESSMENT INFORMATION FLOW

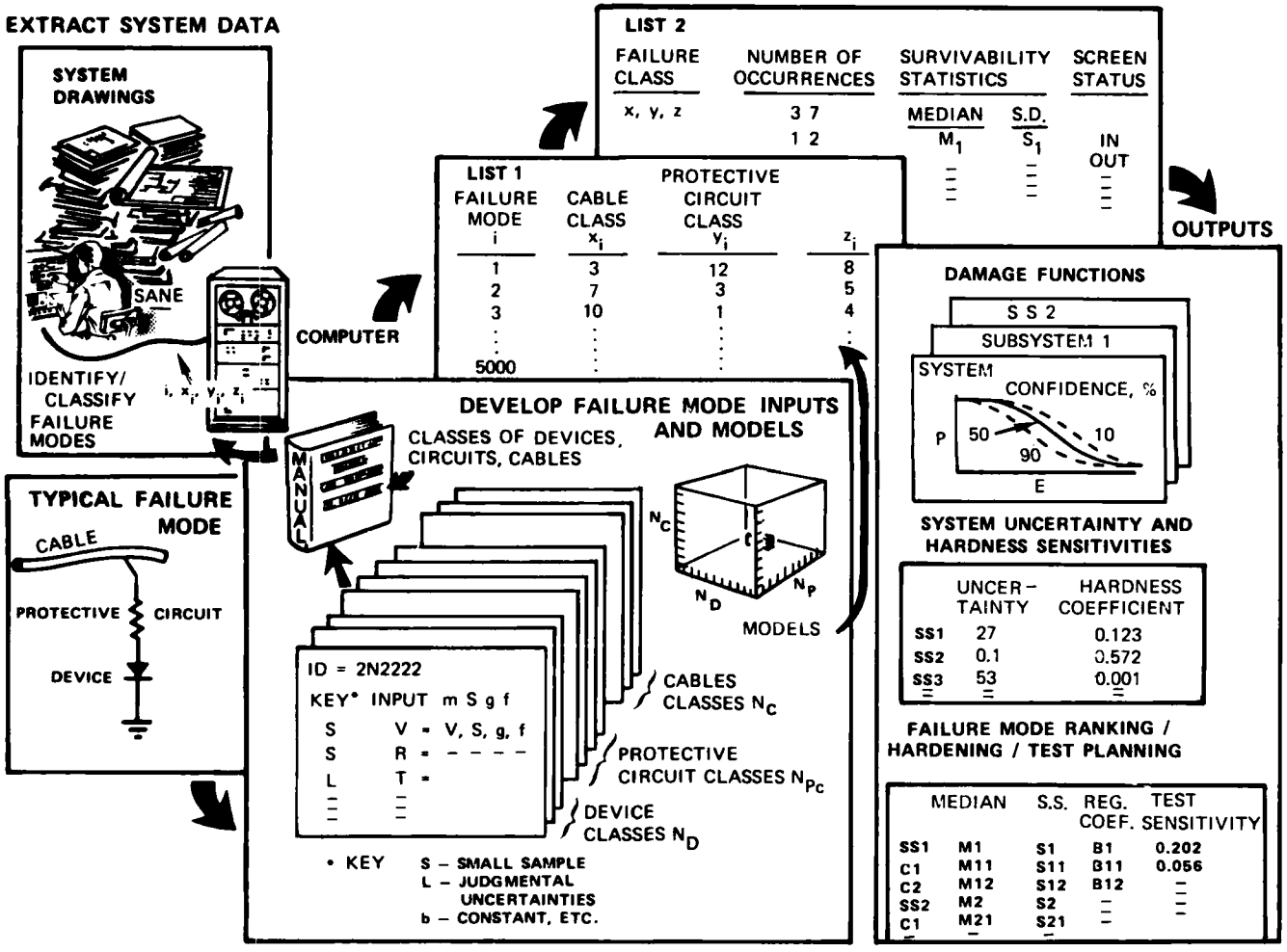

Figure 2.1-1. Overview of the Statistical Management of Preliminary Assessment

In the case of the protective circuits, a definition of a class will include the circuit topology and values of parameters for its components. In the case of cables, the classes will define the cable type and length.

For each failure mode we will also identify the most appropriate failure model which combines the parameter values of the various classes of parameters associated with cable, protective circuitry and vulnerable device.

It is important to notice that even if there may be thousands of individual failure modes, organizing the data base in this fashion involves a reasonably limited amount of effort. Suppose for example that there are 20 classes each for cables, protective circuits, and devices. This will require accumulating data for only a total of 60 different classes. However, as shown by the three-dimensional array for models, these can be combined in $20^3 = 8000$ different ways. Admittedly not all of these may be physically meaningful, but nevertheless the point is clear.

The kind of data to be collected is indicated for the 2N2222 transistor on the front data card of the center panel. For this transistor we need inputs on the reverse breakdown voltage, V_D, the bulk resistance, r_B, and the Wunsch damage constant, k. The statistical input data for such parameters can be in a variety of formats. For example, if test data is available, we may input the sample mean, standard deviation, and number of tests that were used to obtain this data. For this format we keypunch an S in the first column of the input card. Some parameters may be subject to uncertainty but there may exist no test data. Then we keypunch an L in the first column, followed by the name of the variable, its mean, and measures of the uncertainty based upon engineering judgment. Other parameters which are constants will receive a C in the first column, followed by the name and the value for the constant. Other input formats may be desirable and can easily be defined in a similar fashion. In the case of protective circuits, the inputs would include the circuit topology and values for the circuit elements. Naturally some of these circuit elements may be subject to uncertainty, which will be described in the inputs.

When the data base has been organized in this fashion, it is summarized in the form of a manual which is used to support acquisition of the system data. System data can be acquired in a variety of fashions. The best way, of course, would be to acquire it during the system design. In our diagram, however, we suppose we are assessing an existing system. Thus, we must extract the system data from system drawings. Depending upon the complexity of the data, this may be a large job, as suggested by the piles of drawings towering over our data collector in the drawing. His

job is to examine the drawings for each failure mode, determine the appropriate classes for the cable protective circuits and devices of the failure mode, and enter these into the computer.

This is a critical activity of the assessment, and one can imagine the possibility of errors occurring. It appears likely therefore, that in the assessment of complex system, a quality control activity should be instituted to assure a sufficiently low error rate.

The computer will be programmed to tabulate this data, as shown in List 1, Figure 2.1-1. There we have identified classes and failure modes by integers. An alphanumeric identifier will be equally acceptable, and may prove more informative.

The computer will then summarize List 1 into List 2. To do this the computer will count the number of failure modes occurring in each element of the three-dimensional classification array. This may result in a much abbreviated list.

Next, the computer will extract from the data base the necessary input data and the failure model for each failure class. The survivability statistics are then calculated for each failure class. These will be displayed both for a single failure mode and also for the combination of all of the failure modes in the failure class. The method of calculating these survivability statistics will be described in detail below. The survivability statistics will include small sample statistics such as the median, standard deviation, and the effective number of tests. The effective number of tests is derived from the test data on the input parameters, and will be more fully explained in the example in Section 2.2.

The computer will then screen the failure classes. Based upon the survivability statistics for each failure class, the computer will identify the controlling failure classes. The other failure classes affect the system or subsystem damage functions only negligibly, and hence may be deleted from more detailed evaluation in the next, Data Base Improvement phase. The method of screening the failure classes will be described in the example.

The computer will then combine the controlling failure class survivability statistics to obtain damage functions for the system and major subsystems as desired. The damage function is the distribution of fluences that fail the system and is given as a function of statistical confidence.

The computer will then proceed to provide decision-aiding information for planning the data base improvement activities of the next phase. To this end a wide variety of parameters will be ranked for their sensitivity to system uncertainty and hardness.

For example, subsystems may be ranked for their percentage contribution to system level uncertainty. They can also be ranked according to hardness sensitivity coefficients. The method of deriving this decision-aiding information is described in the example.

Test planning inputs will also be generated. As was mentioned the SANE computer code can combine test data on inputs to obtain equivalent test data in the form of small sample statistics for a higher system level. For example, test data on parameters can be combined to obtain equivalent test data at the circuit level. Test data at the circuit level can be combined to obtain equivalent test data at the box level. Box level test data can be combined to the subsystem level, which in turn can be combined to the system level. As a result we can directly measure the benefit of testing done at any of these levels on the uncertainty in the survivability statistics of the system level. When this capability is combined with information on the cost, feasibility, and time requirements for testing at any of these levels, we have a very useful tool to support cost-effective test planning. This kind of information is indicated at the bottom of the output panel in Figure 2.1-1, and its method of calculation will be described in the example which follows.

2.2 SAMPLE STATISTICAL PROBLEM.

Problem Description

The sample problem is to derive damage functions for five mission critical circuits exposed to an EMP environment. By working out this calculation in this small sample, the statistical procedures to be employed in the AVCS assessment using the SANE2 statistical analyses code for the thousands of failure modes that comprise the AVCS will become clear.

Damage Function Model

We require a damage function model* for each circuit of our system. The strength and stress may be expressed in terms of a variety of quantities, including (but not limited to) the threshold current, voltage, or power just needed to cause

*The theory of damage function modeling is presented in W.H. Rowan, "Recent Advances in Failure Analysis by Statistical Techniques," Shock and Vibration Bulletin, Sept 1977, Naval Research Laboratory, Office of the Director of Defense Research and Engineering.

damage, and the response current, voltage, or power due to the EMP threat, respectively. The failure mode is the burnout of a semiconductor junction. In order to compare an event at a microscopic level (i.e., burnout) to the environment incident on the system, the model must translate either threshold and/or threat to a common physical point. Common choices of this point are:

- External to the system: propagate the threshold quantity out through the system to obtain the level of the environment which causes failure, then compare to threat environment,
- At the part: propagate the environment down through the system to obtain the response level delivered to the part, then compare to the part threshold,
- At the pin: propagate environment down to and threshold up to the connector pin on an electronics box, then compare.

In the following example the point of comparison is at the part (or equivalently at the pin since we will assume that the vulnerable part is installed at the pin without intervening circuitry).

Next, we postulate the model using peak voltage as the measure of response.*

First, express the relationship between an external electric field and the EMP voltage at the end of a cable as the product of transfer functions, i.e.,

$$V_E = T_1 T_2 T_3 E_0 \qquad (2.2\text{-}1)$$

where

E_0 = peak electric field strength

T_1 = bulk external surface current/external electric field

T_2 = cable shield current/bulk external surface current

T_3 = cable voltage/cable shield current (transfer impedance).

This voltage V_E is, then, the local measure of stress. In a real system we would expect the mean values of some, or all, of the functions T_1, T_2, T_3 to vary from circuit to circuit as a result of configuration variations in cable type, dimensions, and lay.

*The EMP modeling follows that of: C.E. Wuller, "Missile EMP Safety Margins," TRW, 4733.4.79-004, January 1979.

To model the local threshold or failure voltage, assume each cable has terminal protection in the form of back-to-back Zener diodes. Choose the reverse biased diode as the failure mode. The failure voltage is given by

$$V_F = V + I_F R \tag{2.2-2}$$

where

V = the diode's breakdown voltage

R = its bulk resistance

I_F = the current at failure.

Next, we construct a conventional device power model for the failure current.* The failure power is given by

$$P_F = I_F V + I_F^2 R \tag{2.2-3}$$

and can be equated to the Wunsch-Bell parameter of square pulse failure data

$$P_F = K\tau^{-1/2} \tag{2.2-4}$$

where

K = the damage constant

τ = the pulse width.

Equating (2.2-3) and (2.2-4) and solving for the failure current yields

$$I_F = \frac{-V + \sqrt{V^2 + 4R\,K\tau^{-1/2}}}{2R} \tag{2.2-5}$$

*Such models are discussed in R.A. Croxale and A.K. Thomas, "Subsystem Nuclear Vulnerability Assessment Methodology," TRW, 20.3-A018, March 1977.

Then, substituting back into (2.2-2) the failure voltage becomes

$$V_F = \frac{V + \sqrt{V^2 + 4R\ K\tau^{-1/2}}}{2} \qquad (2.2\text{-}6)$$

This failure voltage, V_F, is then, the measure of the strength of the circuit. Note the dependence of V_F on the device parameters of a given circuit.

Finally, we define the circuit safety margin as

$$M = \frac{V_F}{V_E} \qquad (2.2\text{-}7)$$

Subsequently, we will want to linearize (2.2-7). Frequently this is facilitated by working in log-space. Converting the above yields

$$m \equiv \ell n\ M = \ell n\ V_F - \ell n\ V_E \qquad (2.2\text{-}8)$$

Note that with this definition of safety margin we have made $m \leq 0$ the criteria for burnout. The question of whether this criteria is accurate can only be answered by testing.

The Statistical Model

Our objective now is to derive a statistical model for probability of damage. An overview of the statistical development is shown in Figure 2.2-1. In that figure the physical model derived above is shown. We will linearize this model. To accomplish this for the sample problem we will use the linear terms of a Taylor series expansion, although the SANE2 code employs a numerical method for accomplishing the same end.

We will also require test data on the statistical inputs. The format is shown in the lower left of Figure 2.2-1. Suppose we are testing to obtain data on a certain transistor, say 2N2222. We select a transistor at random and measure its reverse current breakdown voltage, V, its bulk resistance, R, and its Wunsch parameter K. We thus have a vector of three numbers for this particular transistor. We repeat this process a certain number of times, each time obtaining a vector of the three measured values. We have obtained a sample of test data. Such data can be analyzed to obtain the

STATISTICAL MODEL OVERVIEW

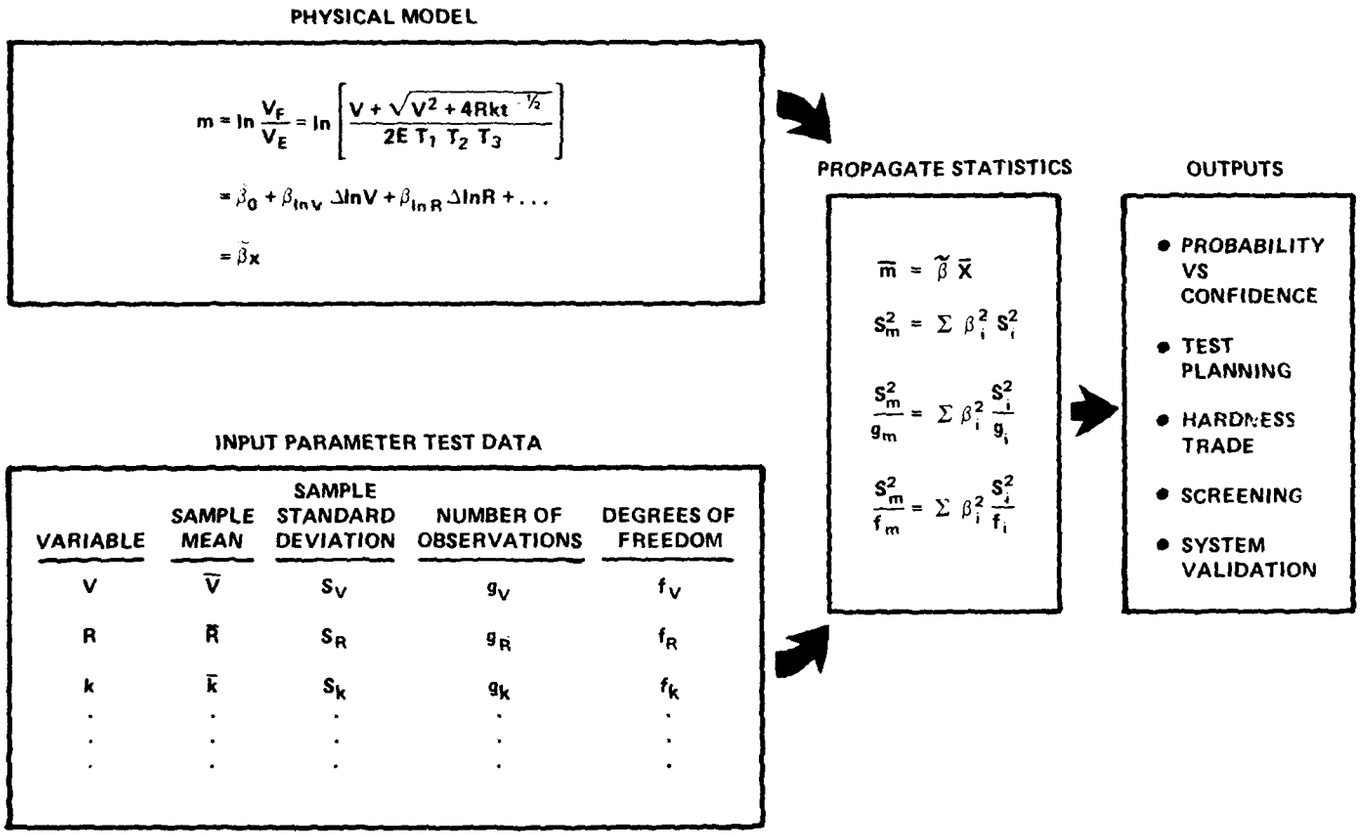

Figure 2.2-1. Information Flow for Statistical Analysis in Preliminary Assessment

mean and sample covariance matrix. In this sample calculation we shall neglect correlations. The panel at the lower left in Figure 2.2-1 shows the resulting data, including the sample mean and sample standard deviation for the three variables. The two right hand columns in that panel show the amount of test data, or sample size, used to obtain the mean and the standard deviation. The number of observations, g, is the number of tests used for estimating the mean; and the degrees of freedom, f, are the number of tests available to estimate the standard deviation. In general, g and f need not be related. The small sample statistics then consist of the four statistics, mean, standard deviation, number of observations, and degrees of freedom. More generally we could include the correlations between the input variables, but these are being neglected for this sample calculation.

We now propagate the input small sample statistics through the linearized physical model to obtain small sample statistics at the circuit level. The equations are shown in a center block of Figure 2.2-1. The four equations shown there permit us to calculate the small sample statistics for a circuit, based upon test data on the input parameters. Our method thus provides us with two alternatives for obtaining circuit level test statistics: 1) we can test the input parameters to a circuit and derive test statistics at the circuit level, or 2) we could test the circuit directly, thereby obtaining test statistics. The choice between the alternatives can be based upon economic and feasibility considerations. It is most important to recognize that while in this example we are combining input parameter test data to obtain circuit test statistics, the same approach can be used at other levels, such as testing at the box or subsystem levels and integrating the resulting test statistics up to the system level. A full discussion of test planning based upon such alternatives is beyond the scope of this report.

Having obtained the small sample statistics at the circuit or system level, we can then proceed to use these for obtaining the outputs shown at the right in Figure 2.2-1. In this report we will briefly indicate how two of these outputs can be obtained.

We will now derive the statistical model for probability of damage, i.e.,

$$P_D = \text{Probability of Damage} = \text{Prob}\ (m \leq 0) \tag{2.2-9}$$

By use of Eq. (2.2-8) this becomes

$$P_D = \text{Prob}\ (\ell n\ V_F \leq \ell n\ V_E) \tag{2.2-10}$$

In Eq. (2.2-10) note that V_F and V_E are treated as random variables, since we assume inputs such as transfer functions and diode characteristics are random.

To evaluate P_D we will assume that all random input variables are log normally distributed (i.e., their logarithms are normally distributed). We assume test data exists from which we can estimate the mean and standard deviations for each input distribution (for this sample calculation we will neglect possible correlations between inputs). Since we have only a limited amount of test data the estimates of the input means and standard deviations may be regarded as random variables distributed about the true, but unknown, population values. A method of treating distributions with uncertain parameters is the method of small sample statistics which we will get to shortly.

The first step in the statistical calculations is to linearize

$$m = \ell n \left[\frac{1}{2}\left(V + \sqrt{V^2 + 4R\, k_\tau^{-1/2}}\right)\right] - \ell n\, E\, T_1 T_2 T_3 \qquad (2.2\text{-}11)$$

which comes from Eqs (2.2-1), (2.2-6) and (2.2-8). This can be accomplished by using the linear terms from a Taylor series expansion. If we apply the small sample statistical treatment to the inputs V, R, k and T_3 we obtain the following truncated Taylor series about the point $(\overline{V}, \overline{R}, \overline{k}, \overline{T}_3)$, the estimates of the means,

$$m = \beta_o + \beta_{\ell nV}\, \Delta \ell nV + \beta_{\ell nk}\, \Delta \ell nk + \beta_{\ell nR}\, \Delta \ell nR + \beta_{\ell n\, T_3}\, \Delta \ell n\, T_3 \qquad (2.2\text{-}12)$$

where the regression coefficients are

β_0 = constant

$$\beta_{\ell nV} = \frac{\overline{V}}{\sqrt{\overline{V}^2 + 4\overline{R}\, \overline{k}_\tau^{-1/2}}}$$

$$\beta_{\ell nk} = \beta_{\ell nR} = \frac{2\overline{R}\, \overline{k}_\tau^{-1/2}}{\sqrt{\overline{V}^2 + 4\overline{R}\, \overline{k}_\tau^{-1/2}}\left(\overline{V} + \sqrt{\overline{V}^2 + 4\overline{R}\, \overline{k}_\tau^{-1/2}}\right)}$$

$$\beta_{\ell n\, T_3} = -1$$

We are now ready to consider small sample statistics on inputs and how these can be propagated through our algebraic model to produce small sample statistics on the

circuit model. An example of small sample statistical inputs is shown in Table 2.2-1. Of the eight input variables, we will treat only four, namely T_3, V, k and R, by the small sample statistical method. Although some of the other variables may be subject to uncertainty, we suppose here that test data to estimate their distributions is not available. Treatment of such variables is beyond the scope of this report and will be discussed in a later report.

Table 2.2-1 summarizes test results on each of the four inputs. The table shows that the transfer function T_3 was estimated by measurements on 10 cables (see column 4) to obtain 10 experimental values for T_3. From those 10 values the sample median 1/32 (column 2), and the sample standard deviation (0.54) of the logarithm of the measured values (column 3) were calculated. Column 4 shows the number of observations, g_i, available for estimating the mean and column 5 gives the degrees of freedom available for estimating the standard deviation. For present purposes then, small sample statistics is limited to the four parameters shown in Table 2.2-1. Our objective now is to combine the input small sample statistics to obtain the corresponding small sample statistics for the circuit (i.e., the distribution of failure probability or damage function).

Table 2.2-1. SANE II Worksheet: Circuit Number 4790685001

Variable	Median	Standard Deviation S_i	Number of Observations g_i	Degrees of Freedom f_i	Regression Coefficient β_i	$\beta_i^2 S_i^2$
E	$5(10)^4$					
T_1	1/10					
T_2	1/270					
T_3	1/32	0.54	10	9	-1	0.30
V	10.6	0.20	10	9	0.14	0.029
k	1.395	1.09	4	3	0.43	0.22
τ	$4.4(10)^{-7}$					
R	0.638	0.16	12	11	0.43	0.005
$\text{Log}_e\ (E_D)$	15.1	0.75	6.3	5.0		
E_D	3.3×10^6					

To calculate the mean for the logarithm of the margin we use Eq. (2.2-12), with mean values of the logarithms (the median) for each of the inputs:

$$\overline{m} = \Sigma\ \beta_i\ \overline{X}_i \tag{2.2-13}$$

where $\overline{X}_i$ = the mean of logarithms the i^{th} variable.

To calculate the variance of the margin we use a result from Reference (18), which states

$$S^2 = \Sigma\ \beta_i{}^2\ S_i{}^2 \tag{2.2-14}$$

To calculate the number of observations for our estimate of $\overline{m}$ in Eq. (2.2-13), we use another result from Reference (18)

$$S_{\overline{x}}{}^2 = \frac{S_x{}^2}{g_x} \tag{2.2-15}$$

where

$S_x{}^2$ = the variance of a parameter x

$S_{\overline{x}}{}^2$ = the variance of an estimate of the mean, $\overline{x}$, based on g_i observations.

From Eq. (2.2-15) we can write

$$S_{\overline{m}}^2 = \frac{S_m^2}{g_m} = \Sigma\ \beta_i^2\ \frac{S_i^2}{g_i} \tag{2.2-16}$$

Equation (2.2-16) can be solved for g_m, the number of observations for estimating the mean $\overline{m}$.

To calculate the degrees of freedom for S_m, we will use an approximation from Reference (19):

$$S_{s_x}^2 = \frac{S_x^2}{2f} \tag{2.2-17}$$

where

$S^2_{s_x}$ = the variance for the estimate of the standard deviation of the parameter x.

From Eq. (2.2-17) we can write

$$S^2_{s_m} = \frac{S^2_m}{2f_m} = \Sigma\ \beta_i^2 \frac{S_i^2}{2f_i} \qquad (2.2\text{-}18)$$

Equation (2.2-18) can be solved for f_m, the degrees of freedom for S_m.

Equations (2.2-13), (2.2-14), (2.2-15) and (2.2-18) provide the small sample statistics for a circuit. The calculations are illustrated in the last two columns of Table 2.2-1. Also, Tables 2.2-2 through 2.2-5 provide inputs and calculation results for four additional circuits.

Damage Functions

Circuit damage functions can be computed from the data in Tables 2.2-1 through 2.2-5. For convenience, the necessary statistics have been collected in Table 2.2-7.

The damage function is the distribution of external field which causes damage. The function can be defined for a single circuit or for a system composed of many circuits. For our present purpose we assume the circuit damage function is a log-normal distribution. Therefore, to define the damage function, we must calculate the mean and standard deviation. The mean is shown in column 2 of Table 2.2-7 and the logarithmic standard deviation is in column 3. Using these parameters, damage functions for each of the five circuits are plotted in Figure 2.2-2, on log-normal probability paper. This paper has the property that log-normal distributions plot as straight lines. The four damage functions are for 50% confidence or best estimate curves. Other confidence levels for the first circuit damage function will be shown later.

Now consider how the damage functions for these circuits might be combined to obtain the "system" damage function. To be done properly, considering the confidence factor, this is best done by the SANE Code because the calculations are rather extensive to be accomplished by hand. An unconservative approximation, using only the 50% confidence curves in Figure 2.2-2 can be done by hand. To do this, pick a damage field strength, E_D, say 10^6 V/M. Read horizontally and obtain the probability 1 - P_D at the

Table 2.2-2. SANE II Worksheet: Circuit Number 4791045002

Variable	Median	g_i = Standard Deviation	g_i = Number of Observations	f_i = Degrees of Freedom	β_i Regression Coefficient	$\beta_i^2 s_i^2$
E	$5(10)^4$					
T_1	1/10					
T_2	1/270					
T_3	1/32	0.54	10	9	-1	0.30
V	90	0.16	20	19	0.64	0.01
k	0.389	1.15	3	2	0.17	0.04
τ	$4.4(10)^{-7}$					
R	4.9	0.34	4	3	0.17	0.003
$\text{Log}_e\ (E_D)$	16.111585	0.59	7.85	6.36		
E_D	$9.935(10)^6$					

Table 2.2-3. SANE II Worksheet: Circuit Number 4720543007

Variable	Median	g_i = Standard Deviation	g_i = Number of Observations	f_i = Degrees of Freedom	β_i Regression Coefficient	$\beta_i^2 s_i^2$
E	$5(10)^4$					
T_1	1/10					
T_2	1/270					
T_3	1/56	0.34	8	7	-1	0.12
V	145	0.23	6	5	0.73	0.02
k	0.279	1.24	4	3	0.13	0.03
τ	$4.4(10)^{-7}$					
R	10.7	0.34	6	5	0.13	0.002
$\text{Log}_e\ (E_D)$	17.0	0.42	6.6	5.49		
E_D	$2.586(10)^7$					

Table 2.2-4. SANE II Worksheet: Circuit Number 4770525

Variable	Median	g_i = Standard Deviation	g_i = Number of Observations	f_i = Degrees of Freedom	β_i Regression Coefficient	$\beta_i^2 S_i^2$
E	$5(10)^4$					
T_1	1/10					
T_2	1/270					
T_3	1/100	0.64	8	7	-1	0.41
V	40	0.34	2	1	0.44	0.02
k	0.076	1.31	5	4	0.28	0.14
τ	$4.4(10)^{-7}$					
R	14.7	0.54	2	1	0.28	0.02
$\text{Log}_e(E_D)$	16.6	0.77	5.82	4.25		
E_D	$1.7(10)^7$					

Table 2.2-5. SANE II Worksheet: Circuit Number 4791045004

Variable	Median	g_i = Standard Deviation	g_i = Number of Observations	f_i = Degrees of Freedom	β_i Regression Coefficient	$\beta_i^2 S_i^2$
E	$5(10)^4$					
T_1	1/10					
T_2	1/270					
T_3	1/18	0.043	10	9	-1	0.002
V	18	0.34	7	6	0.9	0.10
k	0.01	0.016	5	4	0.04	0.005
τ	$4.4(10)^7$					
R	1.0	0.59	7	6	0.04	0.0006
$\text{Log}_e(E_D)$	13.7	0.32	7.04	6.04		
E_D	$9.13(10)^5$					

Table 2.2-6. Screening Example for Sample Problem

Circuit	$\text{Log}_e \bar{E}_D$	S_{E_D}	g	f	$\bar{z} = \text{Log } \bar{E}_D/\bar{E}_r$	s_z	g_z	f_z
1	15.1	0.74	6.27	5.02	1.38	0.81	6.38	5.16
2	16.1	0.59	7.85	6.36	2.38	0.68	7.65	6.37
3	17.0	0.42	6.60	5.49	3.34	0.53	6.75	5.68
4	16.6	0.77	5.82	4.25	2.96	0.83	5.97	4.45
5	13.7	0.32	7.04	6.04		REFERENCE		

Table 2.2-7. Summary of Small Sample Statistics for Sample Problem

Circuit	$\text{Log}_e \bar{E}_D$	S_{E_D}	g	f	P vs C Model
1	15.1	0.74	6.27	5.01	$5.75 = K_p + 1.86\ K_c$
2	16.1	0.59	7.85	6.36	$8.82 = K_p + 2.50\ K_c$
3	17.0	0.42	6.60	5.49	$14.76 = K_p + 4.47\ K_c$
4	16.6	0.77	5.82	4.25	$7.61 = K_p + 2.64\ K_c$
5	13.7	0.32	7.04	6.04	$9.02 = K_p + 2.62\ K_c$

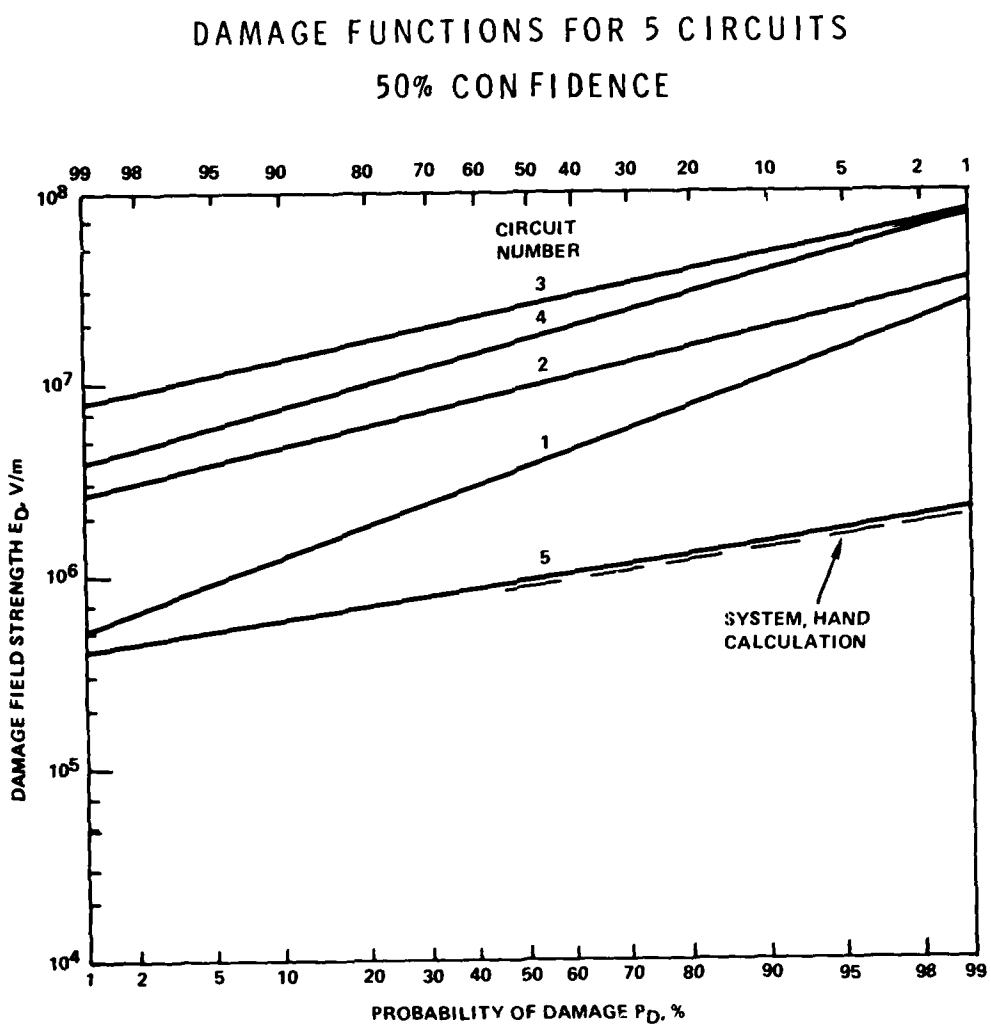

Figure 2.2-2. Damage Functions for Sample Problem, 50% Confidence

top for each damage function. Only circuits 1 and 5 are on scale at this field strength. Take the product of the probabilities:

$$P_1 P_5 = 0.94 * 0.43 = 0.40 = P_{system} \qquad (2.2\text{-}19)$$

which is the probability the system is not damaged at this field strength. This calculation is repeated at several field strengths and the resulting points are connected by a curve, giving the system damage function. The preceding assumed that each

circuit is in series. Circuits are in series if survival of all is required for system survival. Circuits are in parallel if failure of all is required for system failure. The preceding calculation can be adapted for parallel circuits.

Such calculations have been done for the circuit damage function in Figure 2.2-2. The results are plotted as a dashed line for the system damage function. Note that in this case the system damage function differs only slightly from the damage function for weakest circuit. The other four circuits are relatively hard and it may not be necessary to include them in the definition of the damage function. This leads to the concept of screening, which will be illustrated later. Screening of parts of a system from further consideration in an assessment can be important to conserve resources, particularly with systems having large numbers of failure modes.

Probability Versus Confidence Model

We will now consider how small sample statistics can be used for making statements regarding the probability and confidence that can be associated with a wide variety of events.

The salient features of the model are shown in Figure 2.2-3. We shall assume that we are dealing with a parameter that is normally distributed. We have available small sample statistics in the format previously described for estimating the mean and variance of the parameters' normal distribution. Furthermore, there is a certain critical value X_c for the parameter and we wish to determine the probability and confidence that a future value of X drawn from its distribution will exceed the parameter X_c. The parameter X_c may be a design specification or a criteria. Alternatively, our parameter X may be the difference between a strength and a stress, in which case a positive value of X corresponds to survival, and X_c will equal 0. Our approach is quite general and other interpretations are possible.

We wish to determine the separation between X and X_c in units of the sample standard deviation, S, which is required to assure that a randomly selected X from the population will exceed X_c with probability P and confidence C. The exact solution to this problem involves the noncentral t distribution. An approximate solution is available (as follows):

$$\Delta = K_p + K_c \sqrt{1/g + \Delta^2/2f} \qquad (2.2\text{-}20)$$

$$\Delta = \frac{\overline{X} - X_c}{S}$$

PROBABILITY AND CONFIDENCE MODELS

ASSUMPTION

- POPULATION IS NORMALLY DISTRIBUTED
- MEAN AND VARIANCE ESTIMATED BY SMALL SAMPLE STATISTICS

FORMULATION

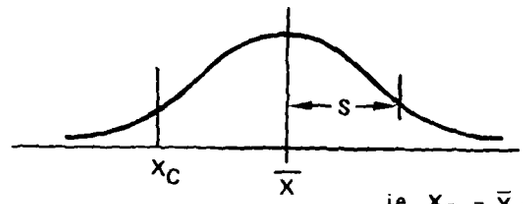

ie $X_C = \bar{X} - \Delta S$

OR $\Delta = \dfrac{\bar{X} - X_C}{S}$

SOLUTION $\Delta = K_P + K_C \sqrt{\dfrac{1}{g} + \dfrac{\Delta^2}{2f}}$

WHERE

$$P = \int_{-\infty}^{K_P} \frac{1}{\sqrt{2\pi}} e^{-\tau^2/2}\, dt$$

$$C = \int_{-\infty}^{K_C} \frac{1}{\sqrt{2\pi}} e^{-\tau^2/2}\, dt$$

P = PROPORTION OF THE POPULATION ESTIMATED TO EXCEED X_C WITH CONFIDENCE C

Figure 2.2-3. Model of Probability vs Confidence

where

$$P = \int_{-\infty}^{K_p} \frac{1}{\sqrt{2\pi}} e^{-t^2/2}\, dt$$

$$C = \int_{-\infty}^{K_c} \frac{1}{\sqrt{2\pi}} e^{-t^2/2}\, dt$$

P = Proportion of the population estimated to exceed X_c with confidence C.

To illustrate the use of Eq. (2.2-20), let us consider the damage function for the first circuit. The 50% confidence damage function for the circuit was shown in Figure 2.2-2, along with the same for the other four circuits. This is replotted in Figure 2.2-4 together with the 10 and 90% bounds for the damage function for the first circuit. To plot the bounds we select a value for the damage field strength, say, $2(10)^6$. The logarithm of this value is inserted as X_c into Eq. (2.2-20). The value for $\overline{X}$ and S are obtained from Table 2.2-1, circuit 1, columns 2 and 3. From the same table we obtain values to insert in Eq. (2.2-20) together with the computed value of delta. We are now free to select values for confidence, i.e., K_c. We shall

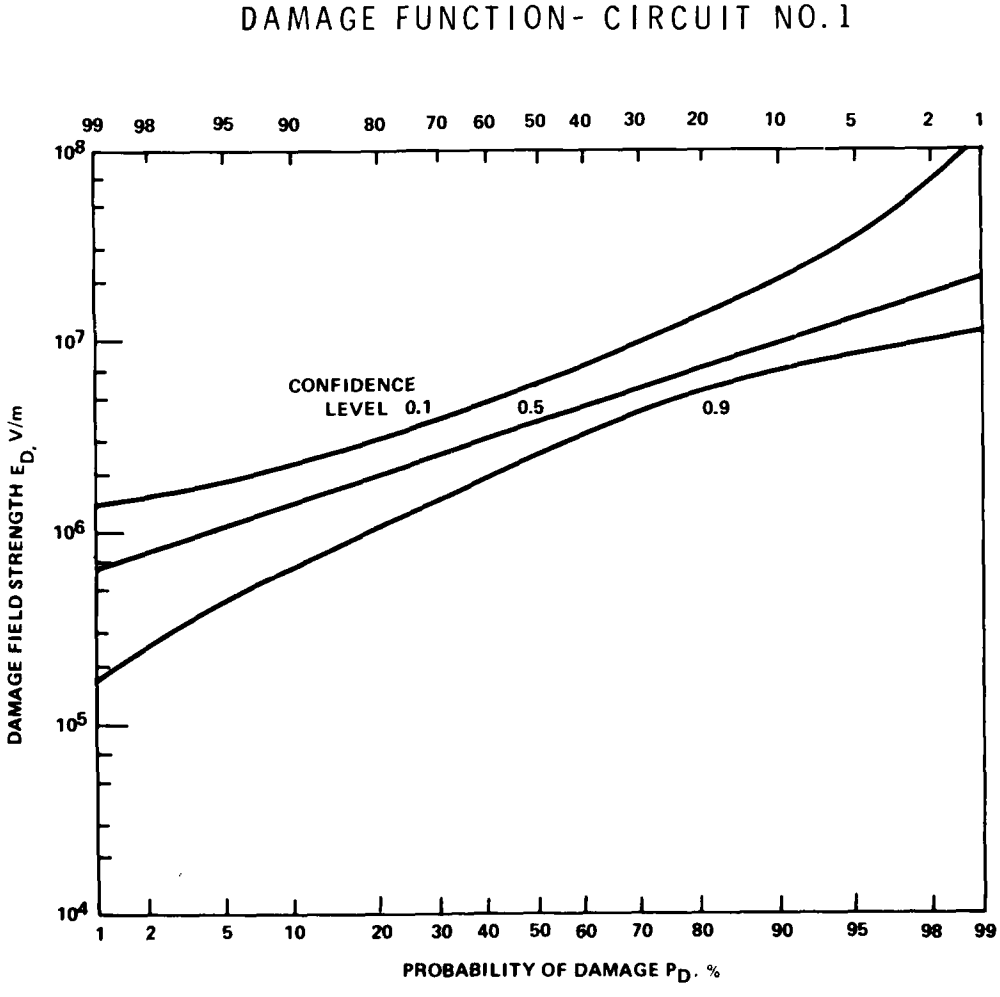

Figure 2.2-4. Damage Function for Circuit One at 10, 50, and 90% Confidence Levels

select 3 values, -1.28 (10% confidence), 0 (50% confidence), and 1.28 (90% confidence). As a result, we obtain three values for P_D, which can be plotted at the corresponding field strength, $2(10)^6$. Continuing this process for other field strengths we generate the three curves shown in Figure 2.2-4. As was already said, the 50% curve is identical with the curve that was previously shown in Figure 2.2-2. The interpretation of the 10 and 90% confidence envelopes is as follows. An infinite number of straight lines can be drawn within these two curves as envelopes. The difference between the curves is that the mean value and the slope or standard deviation have different values. Each of the lines represents a possible true distribution for the damage function for circuit 1. Based upon the small sample statistics that we used, we have an 80% confidence (we lost 10% in each tail) that the true distribution is one of those contained within the envelope.

As another example of the application of Eq. (2.2-20), let us consider the probability and confidence that the strength of each of the circuits exceeds a hypothetical design specification, say a field strength of $5(10)^4$ volts per meter. In this case for X_c we use the criteria value, $5(10)^4$. Then from Table 2.2-1 we obtain the mean, standard deviation, g and f values for each circuit which are inserted into Eq. (2.2-20). This defines all of the parameters in (2.2-20) except K_p and K_c. The results are shown as the final column in Table 2.2-1. We then proceed to plot the relations in Table 2.2-1 on Figure 2.2-5. We find, however, that only the first circuit in on scale, the other four circuits have a probability and confidence both exceeding 99% and hence, do not appear on the plot. The single curve shown in Figure 2.2-5 is for circuit 1.

Screening

Many systems contain a large number of possible failure modes, ranging in the hundreds up to the thousands. It becomes important, therefore, to be able to quickly identify the controlling failure modes. This is useful in design trade studies of new systems, and in a hardness assessment or upgrade of existing systems. Consider now how the screening can be accomplished using the small sample statistical approach.

The first four columns of Table 2.2-6 contain small sample statistics for the five circuits, reproduced from Table 2.2-4. The last four columns of Table 2.2-6 contain small sample statistics for the difference z between the first four circuits and the fifth, which is the weakest (has the lowest mean). Call the damage voltage for the fifth circuit E_r, and let Z be defined as a random variable which is the logarithm of E_D for one of the four circuits, minus the log of E_r. We want to determine the

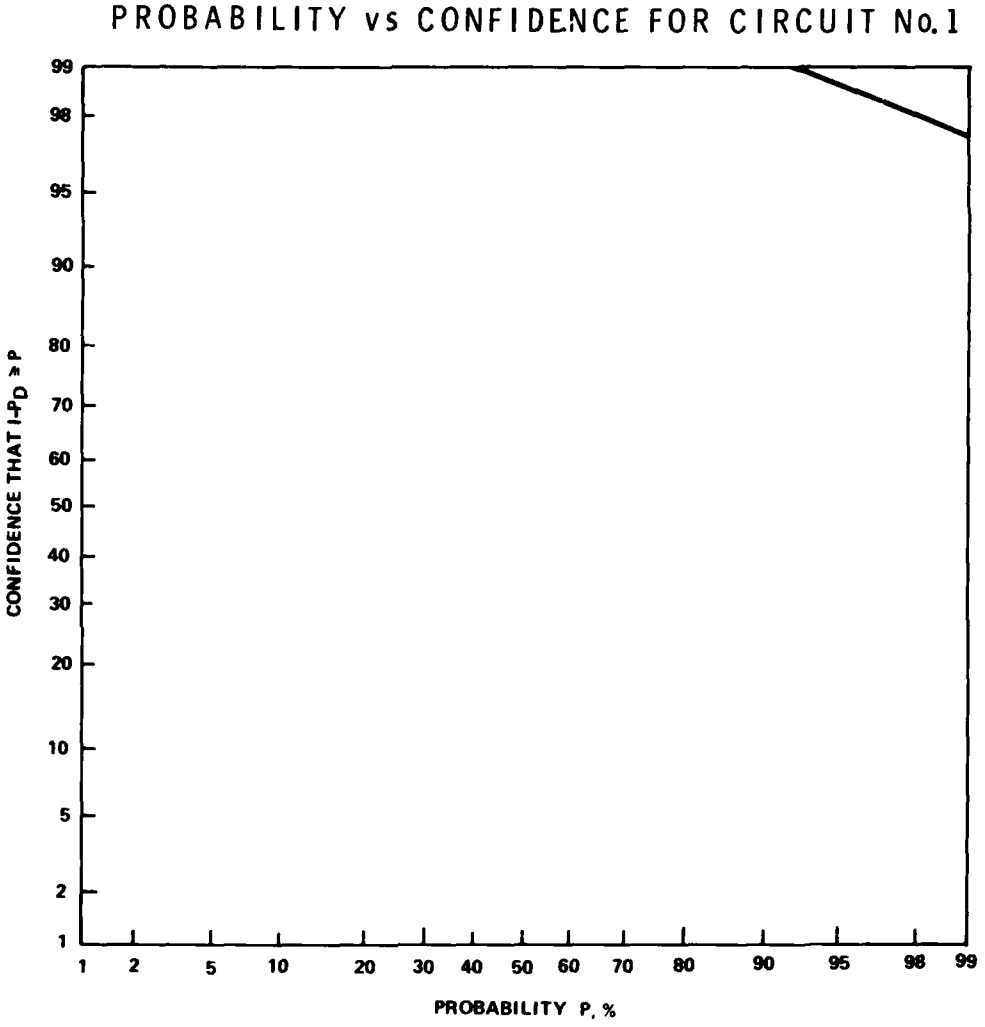

Figure 2.2-5. Probability vs Confidence Model for First Circuit of Sample Problem

probability and confidence that Z exceeds 0. If, for a given circuit, this probability is high with a high confidence, then that circuit could be dropped from the damage function for the system without a significant effect. Note that the new function is already linear, and that we have the small sample statistics for the input, i.e., for each circuit. Thus, we can calculate the small sample statistics for Z by the methods already described. This has been done with the results shown in the last four columns

of Table 2.2-6. The next step is to insert the small sample statistics for each circuit into Eq. (2.2-20), obtaining a relationship between K_p and K_c. The results of this calculation are shown in Figure 2.2-6. The final point is to select some point, a probability and confidence, such that if the curve for any circuit falls above and to the right of that point we will screen the circuit. In general, one might select such a point based upon a consideration of relative costs for more detailed analysis and testing of a given failure mode, compared to the cost of making a screening error. Bearing in mind the very slight effect that the first circuit had on the system damage function in Figure 2.2-2, we suggest tentatively that the 80-80 point be selected. This point has been shown in Figure 2.2-6. Using this criteria, we would screen out all the variables except the fifth.

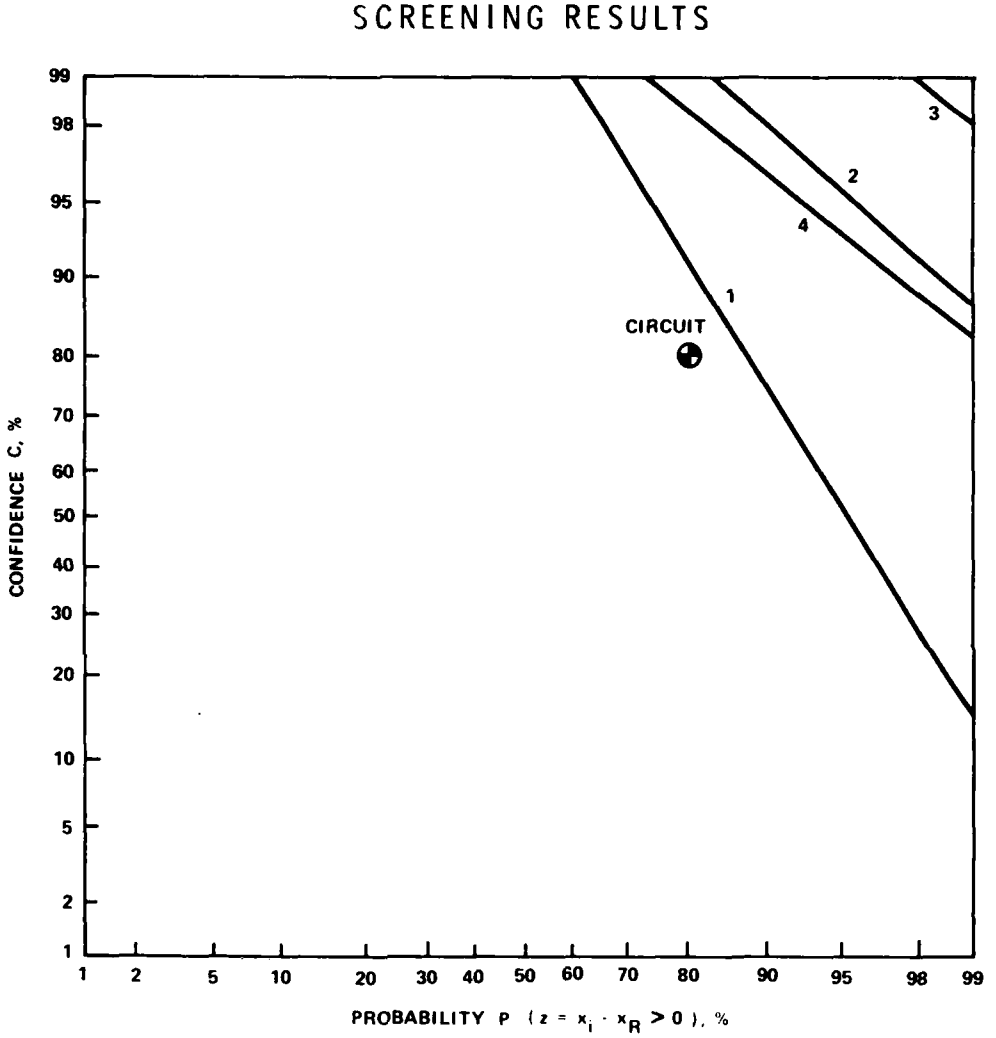

Figure 2.2-6. Probability vs Confidence for Screening

SECTION 3

ASSESSMENT PROCEDURES FOR NUCLEAR WEAPONS EFFECTS

The tasks for the preliminary assessment of the AVCS for each NWE consist of the following:

- gathering data for all failure modes
- classifying data into appropriate categories
- applying appropriate model to obtain damage function and/or probability of survival for a given failure mode.
- documenting the results for each failure mode
- statistically combining the individual failure mode damage functions to yield a system level damage function

This section provides a roadmap for accomplishing all of these tasks (except the last, which was discussed in Section 2). Each NWE is discussed below in terms of

- history of the FLTSATCOM hardening effort, and data obtained in the course of that effort
- formulas and algorithms for calculating damage functions
- assumptions, limitations and uncertainties in the models
- classification of data
- preparation of the failure mode data sheet

3.1 SGEMP BURNOUT.

History of FLTSATCOM Hardening Effort for SGEMP Burnout

The requirement for hardening in the program was that no catastrophic failure of any part (burnout) at a particular X-ray threat level (fluence) was permitted. The basic hardening effort for SGEMP burnout was the following:

- use of individually shielded cabling (braid or semi-rigid) for box-to-box interconnections in order to make direct injection cable response the dominant SGEMP coupling mechanism.
- use EM and X-ray shielded boxes (components), but the overall satellite structure was not designed to be RF-tight.
- painting the inside of FLTSATCOM bays with cat-a-lac paint, a low Z material, to minimize cavity field coupling.

- use of terminal protection, mostly in the form of zener diodes or capacitive filters, to attenuate the SGEMP induced signal.
- use low response cabling (semi-rigid) when terminal protection was not feasible.
- hardness demonstration by analysis only.

The only testing that was done for SGEMP was:

- direct drive X-ray tests of cabling (individual wires, not the entire harness)
- single shot current injection tests of engineering model circuits to verify that terminal protection was working (i.e., shunting the currents)

The analysis that was done calculated the SGEMP current from direct injection expected at the pin, assumed that all of the energy would reach the most vulnerable part, and compared the peak power generated by the threat with the threshold of the vulnerable device, which was exclusively taken to be a semiconductor device. A safety margin was calculated and terminal protection was sized accordingly. Rough estimates of cavity-field coupling and replacement current coupling were also made.

Probably the most uncertain aspect of the hardening effort was the cavity field coupling. The issues here centered around estimating the induced shield currents on the one hand, and estimating the shield-to-core transfer impedance on the other. Since most of the cabling consisted of single-shield hookup wire with relatively large leakage (85% braid coverage), and further, since no transfer impedance measurements were made at the time, the cavity field coupling estimates are suspect.

Since that time the original hardening program data has been supplemented by

- models and test results for direct injection response of cabling

However, the uncertainties in the cavity-field coupling to cables still remain. In addition, it was assumed that synergistic effects such as ionization in the semiconductors would not interfere with the terminal protection.

Finally, some rough calculations were made in order to verify that SGEMP inside boxes (box IEMP) was negligible.

To summarize, the data available from the original hardening program is probably adequate for assessing the SGEMP direct injection response of the AVCS, at least at the criterion environment for which the satellite was designed. For other SGEMP mechanisms, the data is questionable.

Failure Mode Identification

SGEMP energy is coupled into the AVCS through the cabling connected to its components. Accordingly, the box interface pin is used to identify the SGEMP failure mode, even though the actual failure is of a single vulnerable part in the circuit. In the preliminary assessment only direct injection response of cabling is considered. Estimates of cavity field coupling and box IEMP coupling are given at the end of this section in order to justify treating only direct injection response in the assessment.

Damage Functions for Direct Injection SGEMP Coupling

The effect of X-rays on shielded cabling may be reduced to the simple equivalent circuit shown in Figure 3.1-1 (see Ref 8). The peak value of the Norton equivalent I_N is given by

$$I_N = K \begin{cases} \left(1 - \frac{D}{4vt_o}\right) D , & D \le 2vt_o \\ vt_o , & D > 2vt_o \end{cases} \qquad (3.1\text{-}1)$$

$$K = K_{norm}\, \phi / t_o$$

where K_{norm} is the normalized cable source term (C-cm/cal), ϕ is the X-ray fluence (cal/cm^2), t_o is the radiation FWHM pulse width, $v \approx 2/3c$, and D is the cable length. The Norton impedance Z_N is given by

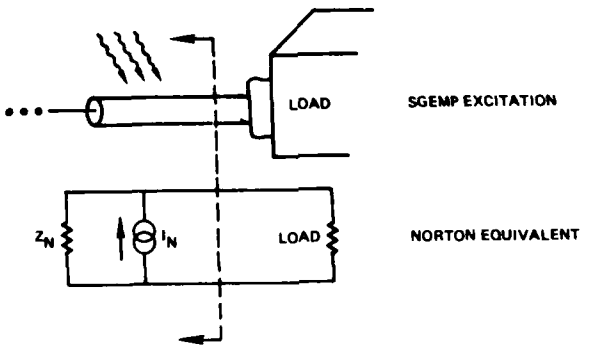

Figure 3.1-1. Definition of an SGEMP Pin Specification in Terms of a Norton Equivalent Circuit

$$Z_N = Z_o \left(1 + \left[\frac{vt_o}{D}\right]^2\right)^{1/2} \qquad (3.1\text{-}2)$$

For purposes of this preliminary assessment we ignore the attenuation of the X-rays through the satellite skin, which is reasonable for a hot X-ray spectrum. Accordingly, the normalized source term K_{norm} which in principle depends on the X-ray spectra, will be evaluated for an energetic X-ray spectrum.

The circuit inside the box is reduced to its most vulnerable semiconductor device on the one hand, and its terminal protection on the other, and attenuation between protection and part is ignored. This is shown schematically in Figure 3.1-2.

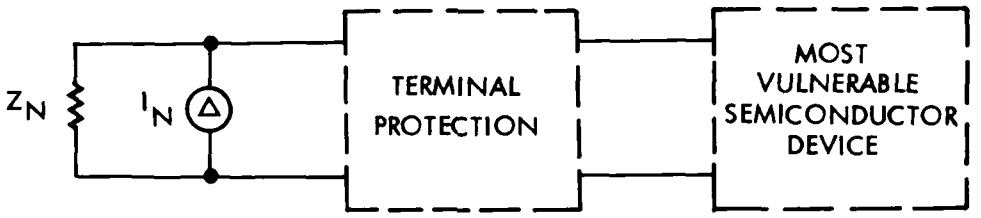

Figure 3.1-2. Equivalent Circuit for Estimating Susceptibility of Circuit to SGEMP Burnout

It is assumed that the most vulnerable device, if it fails, will fail at the junction closest to the pin in question. The effects of being connected to multiple pins which are being driven simultaneously are ignored. It is further assumed that the SGEMP signal drives both the terminal protection junction (if it is a zener) and the vulnerable device into the active region where they are both modeled as bulk resistance in series with a battery whose value is the reverse breakdown voltage. If we allow I_D to represent the reduced current arriving at the vulnerable device due to the attenuation of I_N by the terminal protection, where

$$I_D = \alpha \, |I_N| \qquad (3.1\text{-}3)$$

then the power delivered to the junction is

$$P = I_D^2 \, r_D + I_D V_D \qquad (3.1\text{-}4)$$

where r_D is the bulk resistance of the device, and V_D is the device breakdown voltage. We will compare P with the Wunsch-Bell damage constant in the form

$$P_{damage} = At_{eff}^{-B} \tag{3.1.5}$$

where t_{eff}, the effective pulse width of the signal delivered by the cable, is

$$t_{eff} \approx 2\ (t_o + \frac{D}{v}) \tag{3.1-6}$$

and A and B are empirical constants obtained from pulse-power burnout measurements.[6] By equating P and P_{damage}, and noting that I_D is proportional to free field fluence ϕ, one solves for the fluence-to-fail ϕ_{fail},

$$\phi_{fail} = \frac{-V_D + \sqrt{V_D^2 + 4At_{eff}^{-B} r_D}}{2\alpha[I_N/\phi]r_D}$$

where $[I_N/\phi]$ is the normalized Norton equivalent driver (current/fluence). Formulas for α for the different possible protection schemes are shown in Table 3.1-1. Since the parameters that comprise ϕ_{fail} have a statistical distribution then so will ϕ_{fail}, and, as discussed in Section 2, SANE 2 will generate the damage function (i.e., the distribution) for ϕ_{fail}.

Classification of Data

For purposes of gathering data for SGEMP burnout in the most efficient manner the parameters comprising the damage function are grouped into four categories, namely,

I: threat
II: cable
III: terminal protection
IV: vulnerable device

The parameters which are associated with these categories are shown in Table 3.1-2. Cable source terms and characteristic impedance are indicated in Table 3.1-3.

Preparation of the SGEMP Burnout Failure Mode Data Sheet

The steps for filling in the failure mode data sheet are illustrated in Table 3.1-4 where an example is given. The steps are as follows:

1) By examining the FSC Electrical Schematic Data book, identify the
   - box (unit) number
   - connector number
   - pin number

Table 3.1-1. Attenuation of I_N by Terminal Protection

Terminal Protection	Protection Parameters	I_N Attenuation Factor α
Zener Diode	V_{B_D} = zener breakdown V r_B = zener bulk R	$\alpha = \frac{r_B}{r_D}$
Capacitor Filter	C = capacitance	$\alpha = \left\lvert \frac{\frac{1}{r_B}}{\frac{1}{Z_N} + \frac{1}{r_B} + \frac{jC}{t_o}} \right\rvert$
Series Resistor	R = resistance	$\alpha = \frac{Z_N}{R + r_D + Z_N}$
Back-to-Back Zeners	V_{B_D} = zener breakdown V r_B = zener bulk R	$\alpha = \frac{r_B}{r_D}$
Zener + Resistor	V_{B_D} = zener breakdown V r_B = zener bulk resistance R = resistance	$\alpha = \frac{r_B}{r_D + R}$

- circuit protection class
- vulnerable device: If several devices are candidates, use Table 3.1-5, which reports the power to fail at 1 μsec

2) From the System Interface Document identify the cable type connecting the pin

3) From the FSC Wire List identify the cable length.

Pages of the FSC Electrical Schematic Data Book,[16] System Interface document,[17] and Wire length table[15] are shown in Figures 3.1-3, 3.1-4, and 3.1-5 respectively. These are used in constructing the example of the failure mode data sheet shown in Table 3.1-4.

Table 3.1-2. SGEMP Parameter Categories

Category	Parameters	Source of Information
I: threat	pulsewidth t_o	arbitrary
	spectrum	arbitrary
II: cable	length D	FSC wire length table, Ref 15
	direct injection source term	Table 3.1-3
	characteristic impedance Z_o	Table 3.1-3
III: terminal protection	a) zener: breakdown voltage and bulk resistance	Ref 6
	b) capacitor filter: C	FSC Electrical Schematic, Data Book,Ref 16
	c) series resistor: R	FSC Electrical Schematic Data Book, Ref 16
	d) back-to-back zeners	same as a)
	e) series resistor + zener	same as a) and c)
IV: susceptible device	breakdown voltage,bulk resistance,and damage constant	Ref 6

Table 3.1-3. FLTSATCOM Cables

FSC Cable Type	Specification Number	Characteristic Impedance (Ω)	Cable Source Term at 50 keV K_{norm}((C - cm)/cal)
1S16	3A002-008	3.4	-1.76×10^{-8}
1S20	3A002-006	11.2	-7.93×10^{-9}
1S24	3A002-004	18.8	-4.75×10^{-9}
1S26	3A002-003	26	-3.49×10^{-9}
1S28	3A002-002	33	-2.76×10^{-9}
CX28	3A021-001	50	-2.88×10^{-9}
S141	3A024-002	50	7.98×10^{-11}
SR90	3A024-005	50	-3.07×10^{-8}

Table 3.1-4. Failure Mode Data Sheet for SGEMP Burnout

Unit	Unit No.	Subassembly	Connector Number	Pin No./ Identifier	Cable Class	Cable Length	Terminal Protection Class	Vulnerable Device
AEA	201	SPE	P16	17/RP-BN	1S28	15' 2"	Zener	T^2L

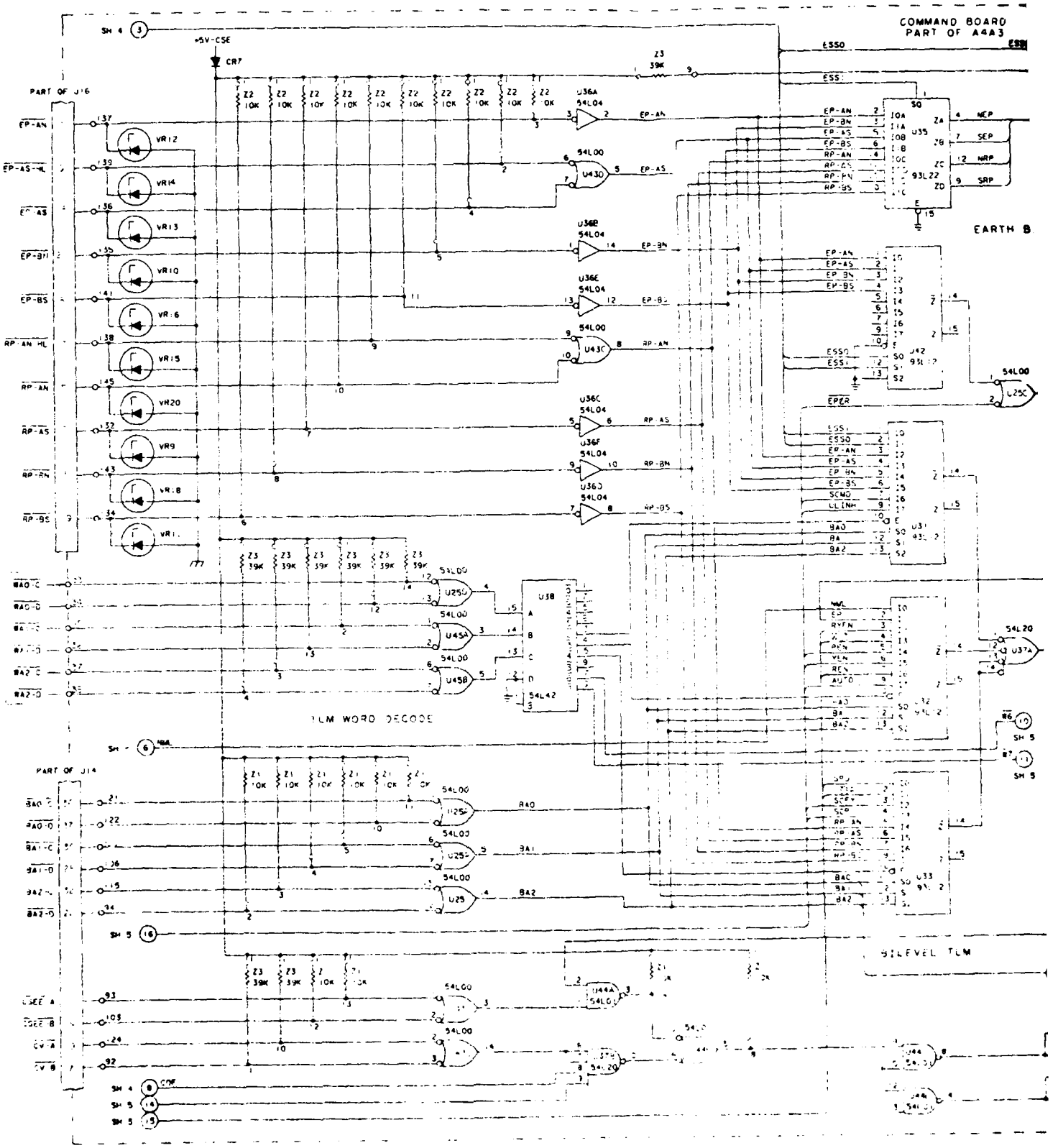
COMMAND BOARD
PART OF A4A3
+5V-CSE
CR7
PART OF J16
EP-AN
EP-AS-HL
EP-AS
EP-BN
EP-BS
RP-AN HL
RP-AN
RP-AS
RP-BN
RP-BS
VR12
VR14
VR13
VR10
VR6
VR15
VR20
VR9
VR8
VR1
U36A
U36B
U36E
U43C
U36C
U36F
U36D
54L04
54L00
EARTH B
ESS0
ESS1
EPER
SCMD
LLINH
BA0
BA1
BA2
TLM WORD DECODE
PART OF J14
U25D
U45A
U45B
U38
54L42
U25A
U25C
U25
54L20
U37A
SH 4
SH 5
SH 6
BILEVEL TLM

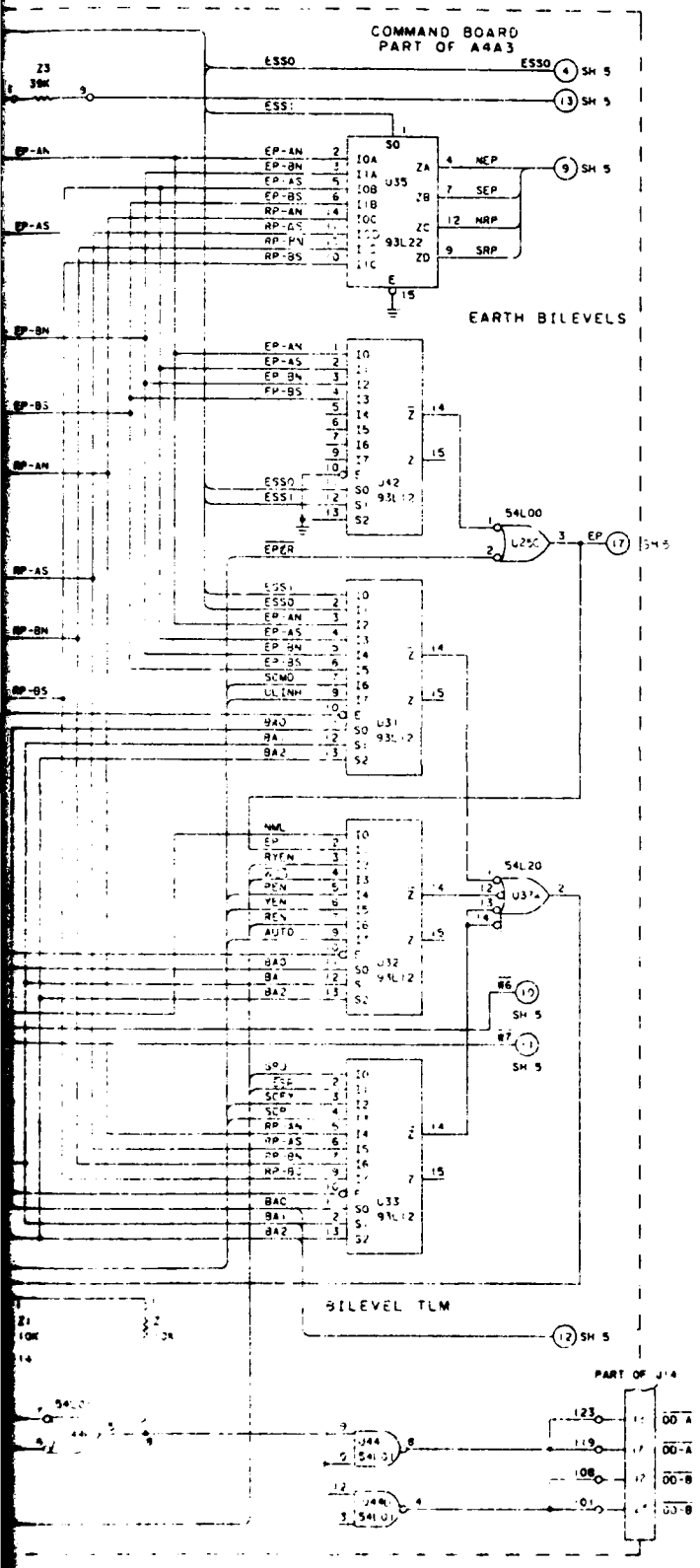

Figure 3.1-3. FLTSATCOM Circuit Schematic: Example

DUAL SPACECRAFT SID C31S219 REV D

SYSTEM INTERFACE DEFINITION

DATE 12/01/75
PAGE 6-11

FROM SUB-SYST	FROM UNIT NO.	FROM SUB-UNIT	FROM CONNECTOR NO.	FROM PIN NO.	LITERAL DESCRIPTION	VIA INTERFACE IDENTIFIER	VIA FUNCTION IDENTIFIER	VIA SIGNAL TYPE	VIA WIRE TYPE	VIA WIRE SIZE	VIA WIRE TWIST CODE	TO SUB-SYST	TO UNIT NO.	TO SUB-UNIT	TO CONNECTOR NO.	TO PIN NO.	REV. NO.
201			P16	5	CMD EXECUTE (CEX BAR)	CABA001			IS 26			301			P12	22	
201			P16	6	CMD VALIDATE (CVAL BAR)	EKBA003			IS 26			011			P07	10	B
201			P16	7	RAD. PRES. A-NORTH HLTP	AABA00B			IS 28			101		J03		3	B
201			P16	8	EARTH PRES. A-SOUTH BAR	BSBA025			IS 28			219		P03		2	A
201			P16	9	RAD. PRES. B-SOUTH BAR	BSBA113			IS 28			219		P05		19	A
201			P16	10	RAD. PRES. A-SOUTH BAR	BSBA022			IS 28			219		P03		19	A
201			P16	11	GND												
201			P16	12	SPARE												
201			P16	13	SPARE												
201			P16	14	GND												
201			P16	15	CMD CLOCK (CCLK BAR)	EKBA004			CX 28			311			P07	20	C
201			P16	16	RAD PRES A NORTH BAR	BSBA021			IS 28			219		P02		19	
201			P16	17	RAD. PRES. B-NORTH BAR	BSBA118			IS 28			219		P06		19	A
201			P16	18	EARTH PRES. B-SOUTH BAR	BSBA101			IS 28			219		P05		2	A
201			P16	19	EARTH PRES. A-SOUTH HLTP	AABA00B			IS 28			101		J03		1	B
201			P16	20	EARTH PRES. A-NORTH BAR	BSBA024			IS 28			219		P02		2	
201			P16	21	EARTH PRES. B-NORTH BAR	BSBA116			IS 28			219		P06		2	A
201			P16	22	GND												
201			P16	23	SPARE												

SYSTEMS 4071

Figure 3.1-4. FLTSATCOM System Interface Document: Example

WIRE LENGTH TABLE

FROM UNIT	TO UNIT	LENGTH
201	124	7.7
201	156	5.8
201	201	1.0
201	201	1.0
201	202	2.6
201	207	13.7
201	211	13.0
201	212	13.3
201	213	13.8
201	214	11.2
201	217	14.3
201	218	8.0
201	219	16.2
201	220	11.6
201	221	18.3

Figure 3.1-5. FLTSATCOM Wire Harness Lengths: Example

Estimate of Cavity Field Coupling

The hardening effort on FLTSATCOM to reduce the effects of cavity field excitation on cables was to coat the interior of the satellite with cat-a-lac paint, a low-Z material, in order to minimize electron emission, and to employ shielded cabling. No specific criteria for shielding effectiveness, for the purpose of making cavity field coupling less than direct injection response, were imposed.

The detailed physical models which might be used for coupling calculations have not been developed to the point of supplying validated engineering models for estimating coupling to cables. Accordingly the formalism developed here, which is based on Ref 12, has substantial uncertainties. We assume, for example, that a quasi-static picture describes E- and H-field coupling and therefore that E and H fields are decoupled, even though the validity of this assumption has not been demonstrated.

Electric Field Coupling to Shields

The effect of electron emission from a surface is to produce a dipole layer of charge whose static E-field couples to system cabling. The current/length K_E induced on a shield by E-field coupling (see Figure 3.1-6) is given by

$$K_E = C' \frac{dV}{dt} \qquad (3.1\text{-}7)$$

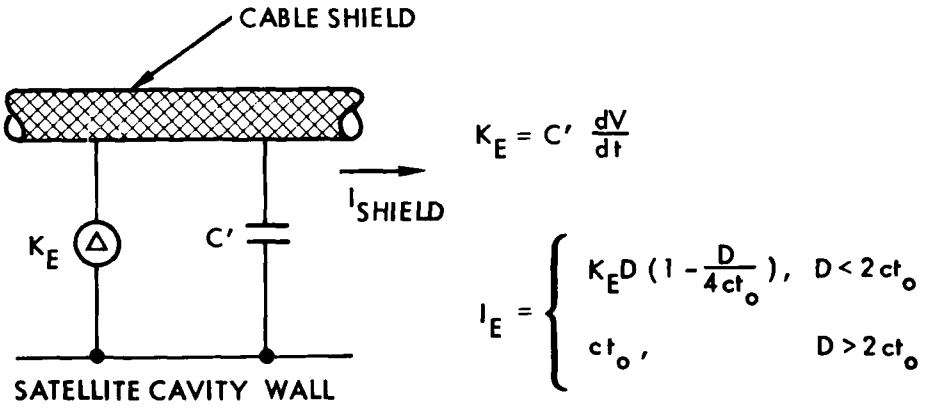

Figure 3.1-6. Electric Field Coupling Model

where C' is the capacitance/length of wire of diameter d a distance h above a ground plane

$$C' = \frac{2\pi\varepsilon_o}{\cosh^{-1}\left(\frac{2h}{d}\right)} \tag{3.1-8}$$

$\frac{dV}{dt}$ is the time derivative of voltage at the cable

$$\frac{dV}{dt} = \frac{E_1 h}{T_p} \tag{3.1-9}$$

h is the height of cable above ground plane (m) (3.1.10)

E_1 is the characteristic E-field from electron emission (V/m)

$$E_1 = 9 \times 10^{-5} \left[\bar{E}\ Y\ R_1\right]^{1/3} \frac{V}{m} \tag{3.1-11}$$

$\bar{E}$ = average electron energy (keV) (3.1-12)

Y = electron yield (electrons/cal) from cat-a-lac for 20 keV photons (3.1-13)

$$Y = 4.5 \times 10^{10}$$

R_1 = flux rise rate ($cal/cm^2/sec^2$) = $\frac{\phi}{t_o^2}$ (3.1-14)

ϕ = fluence (cal/cm^2)

t_o = FWHM of assumed triangular X-ray pulse (sec) (3.1-15)

T_p = time for limiting to occur (sec) (3.1-16)

$$T_p = 0.7 \left[\frac{\sqrt{\bar{E}}}{Y\ R_1}\right]^{1/3}$$

The net shield current induced by the electric field coupling is obtained from K_E by

$$I_E = K_E \begin{cases} D\left(1 - \frac{D}{4ct_o}\right), & D < 2ct_o \\ ct_o, & D > 2ct_o \end{cases} \qquad (3.1\text{-}17)$$

Magnetic Field Coupling to Shields

For the calculation of the magnetic field coupling the loop formed by the cable and the panel wall to which it is grounded is shown in Figure 3.1-7. A cylindrical column of current of radius r_o produces a magnetic field B of magnitude

$$B = \frac{\mu_o J_1 r_o}{2} \qquad (3.1\text{-}18)$$

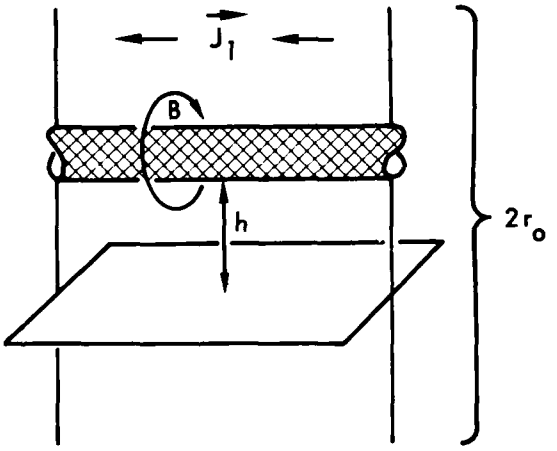

Figure 3.1-7. Magnetic Field Coupling

Here J_1 is the net space charge limited current density accounting for the net current emitted from the satellite walls,

$$J_1\left(\frac{A}{M^2}\right) = 1.1 \times 10^{-15}\left[\sqrt{E}\,Y^2\,R_1^2\right]^{1/3} \qquad (3.1\text{-}19)$$

r_o will be taken as half the maximum cavity dimension, namely r_o = 1m. The amplitude of the induced shield current is

$$I_B = \frac{Bh}{L'} \ , \ L' = \frac{\mu_o}{2\pi} \cosh^{-1} \frac{2h}{d} \qquad (3.1\text{-}20)$$

where h is the height of the cable above the ground plane, and d is the wire diameter. For FLTSATCOM the assume values of h and d are

$$h = 5 \text{ cm}$$

$$d = 0.1 \text{ cm}$$

L' in this instance represents the inductance/length of the transmission line consisting of the shield of diameter d a distance above a ground plane.

Direct Drive of Cable Shields

The induced current/length for charge deposited directly on the shield of cables having been emitted from the wall directly beneath it is given by

$$K_{DD} = J_1 d \qquad (3.1\text{-}21)$$

where d, the cable diameter = 0.1 cm, and J_1 was given in Eq. (3.1-19) above. The net current on the cable is estimated to be

$$I_{DD} = K_{DD} \begin{cases} D\left(1 - \frac{D}{4ct_o}\right) , & D > 2ct_o \\ ct_o , & D < 2ct_o \end{cases} \qquad (3.1\text{-}22)$$

Shield-to-Core Coupling

A rough estimate of the induced core current I_c induced by a shield current I_{shield} acting through a transfer impedance of magnitude Z_T and the dominant frequencies of excitation is given by[13]

$$I_c = I_{shield} \frac{Z_T D}{2Z_o} \qquad (3.1\text{-}23)$$

This expression is valid where the core is terminated in its characteristic impedance Z_o at both ends, and the cable length D is short with respect to the dominant wavelengths of the pulse. A pulse of width 20 ns corresponds to a distance of approximately 6m, while the average length of cable in FLTSATCOM is D < 2m, suggesting that the above formula is reasonable. The AVCS employs braided hookup wire with $Z_o \approx 10\Omega$ and $Z_T \approx 0.2\ \Omega/m$ at 20 MHz, based on measurements from Ref 14 on FLTSATCOM braided 20 and 28 gauge cable.

Using these values in the above formula

$$I_c = 0.02\ I_{shield} \qquad (3.1\text{-}24)$$

Comparison of Cavity Field Coupling Estimates with Direct Injection

The formulas derived above are used to estimate the core wire current from the various SGEMP coupling mechanisms for an X-ray fluence of 1 cal/cm^2, and pulse width t_o = 20 ns. The cable's length is 2m, its diameter is 0.1 cm and it is located 5 cm above the ground plane which is coated with carbon for purposes of calculating electron emission. The core current from cavity field coupling is taken to 0.1 I_{shield}, which is more generous than 0.02 I_{shield} derived in Eq. (3.1-24). The maximum cavity dimension is 100 cm.

The following comparisons are obtained

SGEMP Mechanism	Core Current (A)
direct injection	180
E-field	5
magnetic field	1.1
direct charge deposition	0.1

Accordingly, cavity field coupling will not be included in the AVCS assessment.

Damage Functions for Box IEMP

A direct coupling mechanism for SGEMP excitation within a box occurs from electrons emitted from the box walls and circuit boards, as shown in Figure 3.1-8. For FLTSATCOM the AVCS boxes are coated with 2-3 mils of cat-a-lac paint to reduce electron emission, and the fiberglass circuit boards are coated with 30 mils of polyurethane. Both of these materials are predominantly carbon, and will be treated as such for the purposes of calculating the net electron emission J_{NET}. Assuming that

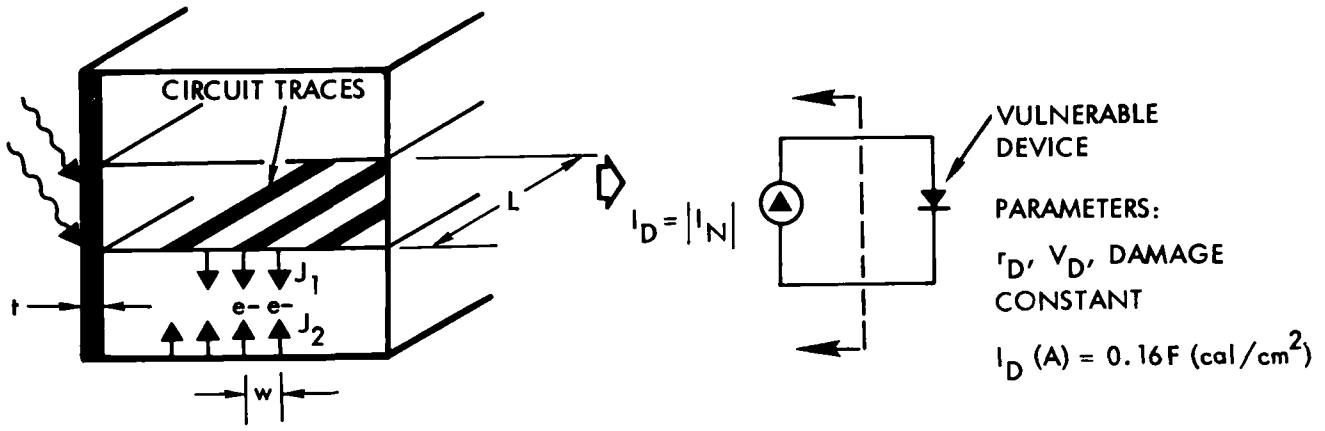

Figure 3.1-8. Box IEMP

all the electrons traveling within a distance w on either side of a circuit board conductor trace contribute their entire amount of charge to the replacement current along that trace, the maximum contribution to the Norton Equivalent I_N in Figure 3.1-1 is estimated to be

$$I_N = (J_1 - J_2)\, wL = J_{NET}\, wL \qquad (3.1\text{-}25)$$

where w could be the distance between two traces on the same board, or the separation between two boards, and L is the maximum box dimension. For this assessment w will be taken as 2 cm and L = 20 cm. The net peak emission current density J_{NET} for carbon at 20 keV for a 10 ns pulse is

$$J_{NET}\left(\frac{A}{cm^2}\right) = 0.16\ \phi\left(\frac{cal}{cm^2}\right) \qquad (3.1\text{-}26)$$

based on a net nonspace-charge limited emission yield from Dellin and MacCallum tables[11] of 2 x 10^{-5} electron/photon. This represents the emission after the free field fluence ϕ was attenuated by 60 mil of aluminum satellite skin thickness as well as box thickness. Inserting the values of L and w mentioned above

$$I_N\ (Amp) = 6\phi\left(\frac{cal}{cm^2}\right) \qquad (3.1\text{-}27)$$

This compares to 180ϕ amp for direct injection using the earlier example. However, note that while the excitation of a circuit trace is equivalent to exciting a pin for the coupling to cables outside the box, in this case there is no intervening protection circuitry between the part and the pin. For this reason Box IEMP is included in the assessment. For purposes of calculating susceptibility (fluence to fail, ϕ_{FAIL}) of the most vulnerable part, $I_N = I_D$ in Eq. (3.1-3) and Table 3.1-1, and $Z_N = \infty$.

3.2 TREE BURNOUT.

History of FLTSATCOM Hardening Effort for TREE Burnout

The hardening effort concentrated chiefly around placing current limiting resistance in the leads of all semiconductor devices. The magnitude of the resistance was at least one ohm per volt of power supply to the device in question. In some RF circuits inductance was used in place of resistance.

The analysis used to verify that the current limiting was sufficient was simply to compare the maximum power that could be transferred to the device in a matched load configuration, $V_{cc}^2/(4R)$, where V_{cc} is the supply voltage and R is the current limiting, with the maximum continuous power rating P_c supplied by the vendor for the device (see Figure 3.2-1). Since P_c is most likely a "3σ" lower limit on a distribution of power for failure, the FLTSATCOM hardening was probably very conservative.

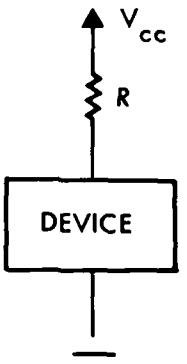

P_c = CONTINUOUS POWER RATING $\geq \frac{V_{cc}^2}{4R}$

V_{cc} = POWER SUPPLY VOLTAGE

R = CURRENT LIMITING RESISTANCE

Figure 3.2-1. FLTSATCOM Analysis for Photocurrent Burnout

The test verification effort centered about 100% lot sampling of parts (5 parts/lot, 300-400 lots) in the TRW Vulcan FXR at dose rates of 10X the criterion environment. The criterion environment in this case was derived from the incident

X-ray flux and its expected attenuation into the boxes. This was probably both reasonable and conservative since the hardening measures themselves are independent of dose rate. On the other hand we observe that this limited amount of testing cannot give significant statistical confidence in hardness.

Failure Mode Identification

The failure mode for TREE burnout occurs at the part level. The failures, if they occur, are taken to be functionally independent, i.e., loading effects are ignored, and parts are treated statistically "in series," i.e., failure of any part fails the system.

Probability of Part Survivability

Consider the radiation response of a diode, as shown in Figure 3.2-2. If the power supply biases the diode in the forward direction, then the effect of the

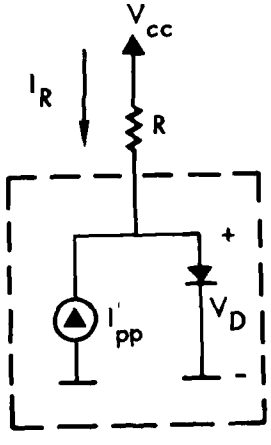

Figure 3.2-2. Equivalent Circuit Model of the Radiation Response of a Diode

photo-current generator will be to drive more current through the ideal diode thus increasing V_D slightly to $V_D + \Delta V_D$ and therefore reducing I_R to $(V_{CC} - V_D - \Delta V_D)/R$. The net power dropped across the device, $I_R V_D$, is therefore only slightly affected by the radiation. In the reverse bias situation where the radiation is insufficient to turn on the ideal diode, the transient photocurrent I_{pp} will buck the dc current V_{CC}/R, making $I_R = V_{CC}/R$ a worst case estimate of the current through R, $V_D \approx V_{CC}$, and V_{CC}^2/R a worst case estimate of the power. This is obviously too high since $V_{CC}^2/(4R)$ is the maximum power transfer. Finally if I_{pp} is large enough to turn on the device, it is possible to get negative power in the device

$I_R V_D \approx - I_{pp} V_D$ (solar cell effect). In any case, it would seem that a worst case estimate of power drops across junctions in semiconductor devices is $V_{CC}^2/(4R)$, a result which is independent of dose rate. This is something of an idealization in some cases since the "R" in an integrated circuit, for example, may be reduced by the radiation environment, giving rise to an explicit dose rate dependence. The amount of uncertainty from this effect is unclear.

Rather than compare the power drop with P_c, the continuous power rating, which is too conservative we will use the Wunsch-Bell damage constant $P_{WB} = At^{-B}$. Since P_{WB} has a known statistical distribution, the percent of the distribution below $V_{CC}^2/(4R)$ is the part's probability of failure.

Classification of Data

The two categories of data for TREE burnout are

I: semiconductor type

II: current limiting configuration (usually V_{CC} and resistance in leads of device)

While there are hundreds of semiconductor devices in the AVCS subsystem there are only a relatively few number of distinct part types. The parameters associated with these categories are shown in Table 3.2-1.

Preparation of the TREE Burnout Failure Mode Data Sheet

The steps for filling in the failure mode data sheet are illustrated in Table 3.2-2 where an example is given. The steps are as follows: By examining the FSC Electrical Schematic Data Book[9], identify the

- box (unit) number
- connector number
- component (i.e., semiconductor part)
- current limiting in each of the leads

Table 3.2-1. TREE Burnout Parameter Categories

Category	Parameters	Source of Information
I: semiconductor type	Wunsch-Bell damage constants	Ref 6
II: current limiting configuration	V_{CC}, lead resistance	Electrical Schematic Data Book

Table 3.2-2. Failure Mode Data Sheet for TREE Burnout

Unit	Unit No.	Subassembly	Connector No.	Pin No./Identifier	Current Limiting Configuration and Part Identification
AEA	201	SPE	P16/J16	17/RP-BN	V_{CC} = 5V R = 10K 54L04 Component

An example of an electrical schematic has already been given in Figure 3.1-4.

3.3 PERMANENT DEGRADATION

History of FLTSATCOM Hardening Effort for Permanent Degradation

FLTSATCOM was hardened against the permanent degradation effects of criteria total doses from neutrons, γ, and fission electrons, with the electron dose representing the most significant threat environment. The effects of short term annealing on circuit operation were not considered specifically since this could be considered in the context of functional upset hardening via fault tolerant design. The obvious hardening approach was to use radiation insensitive parts on the one hand, and circuitry insensitive to parameter degradation on the other.

In order to accomplish the hardening, derating values were obtained for individual part degradation by irradiating parts at some factor above the criteria environments using the C_o^{60} γ source (simulating the ionizing total dose) and a nuclear reactor. 100% lot sample tests, 5 parts/lot were conducted. The average derated parameter values were then used as the design standard by the circuit designers who would define worst case values of the parameters where the circuit in principle would not work, thus establishing a design margin for the circuitry. Unfortunately, how the designer established these worst case values for parameter degradation was not usually documented.

One disconcerting thing from the point of view of our data acquisition was that derating values for n and C_o^{60} irradiation were not reported separately.

Failure Mode Identification

Generally degradation of the individual part is taken to cause failure of the circuit. For some RF applications the entire circuit degradation should be considered, but no such circuits are present in the AVCS subsystem.

Damage Function Analysis for Permanent Degradation from Neutrons

We assume that the free field environment of neutrons is unattenuated to the part under consideration. Let x_i represent the pretest value of a given parameter, x_p the post-test irradiated value. Then the change in parameter as a function of dose ϕ (n/cm^2) is assumed to be given by

$$\frac{1}{x_p} - \frac{1}{x_i} = K_n \phi \qquad (3.3\text{-}1)$$

where K_n is a constant derived from the FLTSATCOM pre- and post-test parameter values. Recall that the FLTSATCOM deratings did not distinguish between damage from n or γ. As a worst case estimate we assume that neutrons were solely responsible for the derated values, and therefore K_n obtained in this way should be fairly conservative. Then if we represent X_{pm} as the minimum (or maximum) acceptable design limit for the parameter (which is provided by the FSC designer in the FSC CDR package[1]) then the failure criterion for fluence is

$$\phi_{fail} = \frac{1}{K_n}\left(\frac{1}{X_{pm}} - \frac{1}{X_i}\right) \qquad (3.3\text{-}2)$$

Since K_n was based on measurements of X_p which have a statistical distribution which is also reported in the CDR package, then ϕ_{fail} also has a distribution which is by definition the damage function.

If a device has several degraded parameters, the minimum value of ϕ_{fail} for all parameters will be employed as the damage function.

Conversion Between Neutrons and X-ray Fluence

Since both X-rays and neutrons are "inverse square" effects, it is possible to convert directly from neutron fluence to X-ray fluence. Therefore, the damage function can be displayed on the same graph as the SGEMP and TREE burnout damage functions.

Damage Function Analysis for Permanent Degradation From Total Ionizing Dose

The same analysis above will apply for total ionizing dose, except $K_n \rightarrow K_\gamma$. In this case, however, the free field environment, which will be represented entirely by fission electrons (ϕ is electrons/cm^2), must be attenuated to the parts in question, which is described below.

The Trapped Radiation Handbook[10] gives a nomograph (Figure 3.3-1) for the depth dose for fission electrons as a function of thickness of aluminum. Now, FLTSATCOM provides 20 mils of aluminum shielding by its satellite panels and 40 mils of aluminum shielding by its electronics boxes. If the X-ray shielding of the boxes is ignored along with the Kovar packaging of the devices, this shielding represents

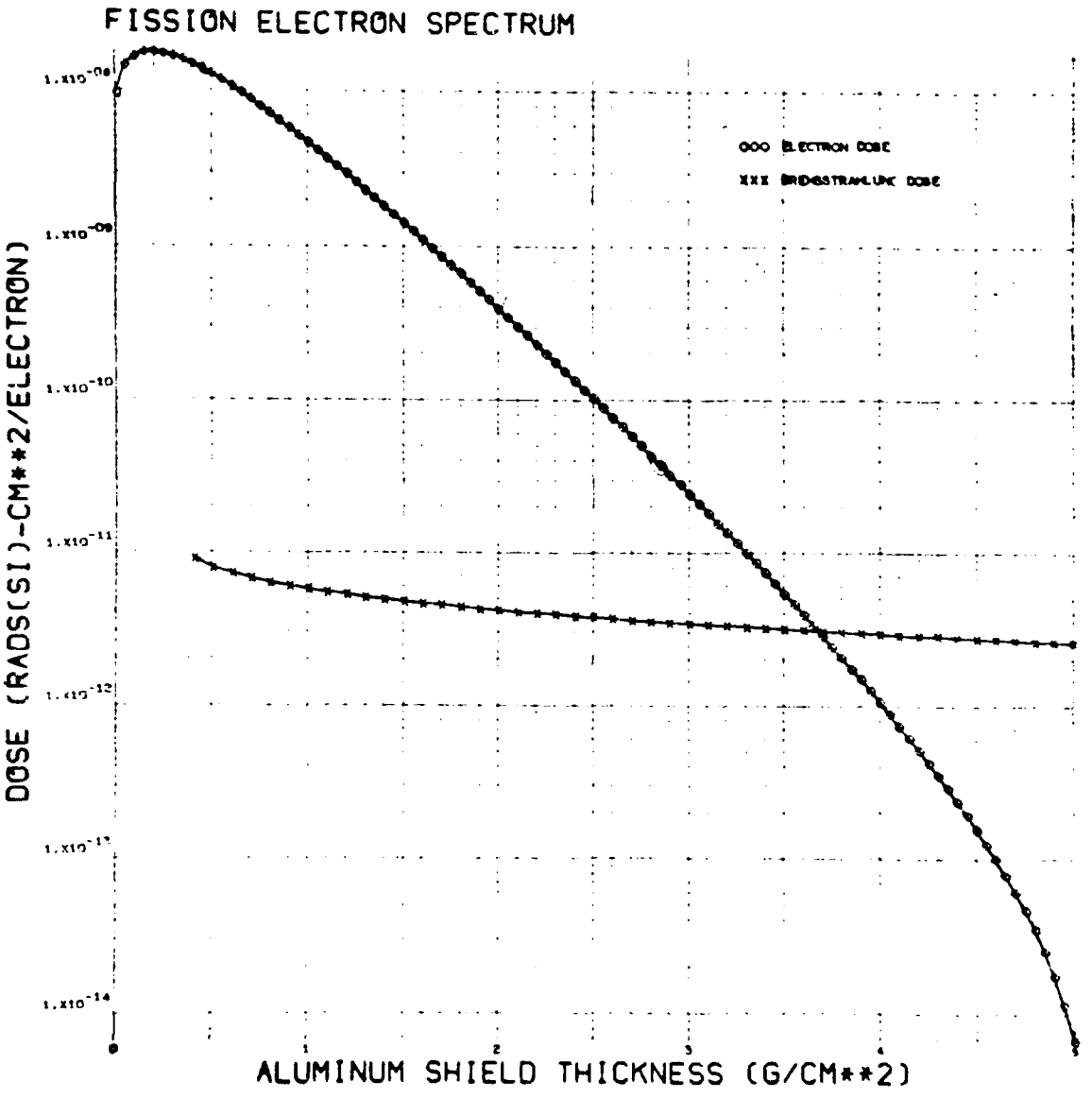

Figure 3.3-1. Depth Dose for Fission Electrons as a Function of Shield Thickness

60 mils x 2.78 g/cm^3 = 0.42 g/cm^2 of aluminum shielding. Using the nomograph (Figure 3.3-1) the conversion factor from free field environment (e/cm^2) to dose at the box is 10^{-8} rads (Si)/e/cm^2. Now one is in position to use the FSC C_o^{60} derating data which were reported in terms of rads (Si), and the damage function can now be plotted as a function of ϕ .

Unfortunately, weapon electrons fluences are not "inverse square" effects, but depend upon the altitude of burst and satellite location in the earth's magnetic field lines, i.e., satellite orbit, as well as yield. Therefore the damage function for total electron dose cannot be arrayed on the same graph as the other damage functions, and will be plotted separately.

Classification of Data

The only class of parameters required to assess damage are a given part's pre- and post-test irradiated values, and the worst-case design limit. This data is provided in the FSC CDR package. The parameters that are likely to be degraded are: β, common-mode rejection ratio, offset voltage, etc.

Preparation of the Permanent Degradation Failure Mode Data Sheet

The steps for filling in the failure mode data sheet are illustrated in Table 3.3-1 where an example is given. By examining the FSC Electrical Schematic Data Book[1)], identify the

- box (unit) number
- connector number
- subassembly
- component

3.4 FUNCTIONAL UPSET

History of FLTSATCOM Hardening Effort for Functional Upset

Functional upset is defined as the presence of a transient due to radiation that causes loss or degradation of a mission critical function. The transient requirements imposed on the performance of FLTSATCOM can be summarized as follows:

a) no change in mode, operational status, or redundancy configuration
b) no change in location or orientation
c) no undesired processing of commands

Table 3.3-1. Failure Mode Data Sheet for Permanent Degradation

Unit	Unit No.	Subassembly	Connector No.	Component
AEA	201	ADE-board 2	J33	LM 108A

d) normal operation restored in X seconds

e) no loss of a bit at operate through level (communication subsystem only)

The transient effects which could prevent these requirements from being met may be due either to irreversible changes in circuitry status or unacceptably long circuit recovery times. In order to identify functional upset failure modes functional analysis was performed to translate the FLTSATCOM performance criteria into specific transient requirements which indicated which circuits had to be hardened to prevent unacceptable transient scrambling and to define allowable circuit outage times to satisfy system requirements. Since a detailed transient analysis of each circuit in the satellite was intractable, an alternative simpler approach was developed, based on the concept of fault tolerant design.

Fault tolerant design as implemented in FLTSATCOM made two basic assumptions. First, since all circuits would be exposed in the same short time interval they would recover in parallel, implying that the recovery time of a given channel would be governed by the recovery times of the circuits with the longest time constants. Thus, only circuits with long recovery times relative to the allowable outage times would require attention. Secondly, it assumed that all circuits that can be upset will upset, regardless of environment level, thereby making the hardening effort independent of both environment and level. The first step in exercising the fault tolerant approach was to perform a functional analysis which translated the transient performance requirements at the spacecraft system-level into requirements at the subsystem and component levels.

In the FLTSATCOM functional analysis, the spacecraft was divided initially into a unique set of functions. Each function was clearly definable in terms of input and output requirements at the system level. This set of functions completely described all spacecraft performance requirements for normal, on-orbit operations. For example, the functions performed by the AVCS include S-band command processing and spacecraft orientation. After the functions were defined, each one was divided into its component functional elements where each functional element was contained within a single electronic box. Next, a failure mode and effect analysis was performed on each function to determine the system effects of transient upsets in the various functional elements. Transient upsets that resulted in unacceptable system performance according to system-level survivability performance requirements were identified for hardening. These data were then used in the development of subsystem and box-level performance requirements.

Failure Mode Identification for Functional Upset

The performance requirements for the AVCS subsystem are shown in Figure 3.4-1. The identification of the functions therein are precisely the failure modes in this assessment.

Data on functional upset verification that the subsystem level transient requirements were satisfied on the AVCS was provided by Flash X-ray testing. In these tests various critical logic states and recovery times are monitored during six shots at either the survive or operate-through level of radiation. The data collected during the FXR tests indicate the parameter value measured for each shot relative to their performance requirements.

Preliminary Assessment Approach for Functional Upset

Since the hardening approach used by FLTSATCOM for functional upset is based on fault tolerant design it seems entirely consistent to also use fault tolerance with its inherent assumptions as the basis of a preliminary assessment methodology. The primary consequence of such an approach is that the functional upset assessment can then be made independent of the environment. This would enable us to use the data generated by the FXR testing of the AVCS to predict survivability of the subsystem to functional upset. Although the assessment approach is as yet still tentative it is envisioned as follows. Associated with each electronic box of the AVCS is a set of values for critical parameters, e.g., recovery times, monitored during the six FXR shots. By using the data associated with the higher survive level radiation one ensures that sufficient energy is delivered to sensitive electronics to upset those circuits which are disturbable. The experimental data for each of the six FXR shots gives a cumulative distribution of sample parameter values. This distribution can in turn be compared with the performance requirements value to obtain the probability that the parameter remains within specification. If one further assumes that all measured parameters contribute independently to the box survivability one can obtain the probability of survival of the box. Similarly, box survivabilities can be combined to yield AVCS function survivability.

Admittedly, the limited data, namely that from only 6 FXR shots, will provide a very limited statistical confidence in the calculated survivability. However, the constraints of the preliminary assessment dictate that it be based only on whatever data presently exists. It should be emphasized that this assessment approach outlined, based as it is on fault tolerant design, will give a probability of survival that is independent of environment.

Function	Functional Element Description
S-Band Command Processing	AVCS Command Decoding This element includes remote decoding matrices located in the AVCS Control Electronics Assembly (CEA) and Actuation Electronics Assembly (AEA). The proper matrix receives the data bits, shift clock, and enable from the command validation and steering element, and shifts the bits into a shift register. In the AVCS decoding elements (three each in the AEA and one in the CEA), the command word is telemetered to the ground for verification and is not executed until a separate execute command processed by the S-band Command Processing function through the EIA decoder, is received by the CEA/AEA decoding elements. Data, clock, enable, and validate lines also go to the UHF Command Decoder, whose function will be described in a later section.
Spacecraft Orientation	Scan Drive and Readout This functional element drives a scanning mirror implemented so that the earth sensor field or view scans across the earth disk. The scan position is also monitored and signals are generated giving the time at mid-scan and at the scan limits. Radiance Detection This element uses a thermistor bolometer to detect the presence of the earth disk from its infrared signal. The earth's horizon is defined by the time the bolometer detects the change from space to earth radiance, and vice versa. Error Computation This element performs the initial earth-pointing-error computation by comparing the earth horizon detection and the scanning mirror position time phasing. The error signal is supplied to the earth sensor processing element for further use. The scan drive and readout, and radiance detection and error computation functional elements are implemented in the Earth Sensor Assembly. Earth Sensor Processing This element operates on the earth pointing errors produced by the error computation element to generate two earth pointing errors, a pitch error and a roll/yaw error. Each of these errors is averaged over a x-second sampling period, and, for the next x-second period, the pitch error is supplied to the wheel control element and the roll/yaw error to the thruster control element.

AVCS Command Decoding

Transients could cause logic scrambling resulting in loss of a command, an acceptable failure mode. If a burst occurs while a command is being decoded an undesired command can be processed, also an acceptable failure mode, because of the low probability of such an occurrence. However, if the decoding matrix outputs can be activated by transient response for a sufficiently long time, an undesired command could be carried out at any time. This failure mode must be prevented.

Scan Drive and Readout, Radiance Detection, and Error Computation

These three elements make up the Earth Sensor, the primary reference sensor for the normal AVCS control mode. Transient upset can occur causing false timing signals, false earth detection signals, or false error signals to be generated. These errors will be propagated through the Spacecraft Orientation function and spurious actions may be taken based on these erroneous signals. The magnitude of the effects of these spurious actions on the spacecraft pointing accuracy depends on the maximum levels and durations of the false error-signals. In general, the errors will persist until the next error sampling operation is initiated, in approximately x second.

Earth Sensor Processing

In the earth sensor processing element, the digital pointing angle error is stored in a register for the x-second sampling time, and is concurrently converted to an analog voltage signal for use by the wheel and thruster control elements. The holding register could scramble due to an event and present a false pointing error to the control laws for up to x second. Response to a false pointing error signal could cause a real pointing error to be introduced. A worst case failure mode could be hypothesized as follows: a burst occurs as the data are being transferred from the error computation to the earth sensor processing element, scrambling both the error computation shift register and the sensor processing holding register; the holding register erroneous data will be supplied to the control elements for x second, then the residual error from the shift register will be transferred to the holding register for the next x-second period. Thus, a false error signal could persist for up to x seconds. The preceding analysis has shown that this x-second error time is acceptable.

AVCS Command Decoding

Transients in the command decoding elements shall not cause the processing of a command during the time that no command is being transmitted; however, the hardening of command storage registers in order to avoid register upset during the time that a command is being transmitted and processed is not required.

Scan Drive and Readout, Radiance Detection and Error Computation

Transients in the ESA electronics shall have subsided in such time that only one sensor-sampling time period shall contain erroneous data.

Earth Sensor Processing

Transients in the Earth Processing Electronics (EPE) shall have subsided in such time that only one earth-sensor sampling period shall be directly effected. In the case where an event occurs during the time when data is being transferred from the ESA to the EPE, then two ESA sampling time periods may be affected.

Figure 3.4-1. Failure Mode Data Sheets for Functional Upset of AVCS

Function	Functional Element Description
Spacecraft Orientation	**Wheel Control** This element implements the pitch axis control laws. The pitch error input operates through the control transfer function and causes a wheel speed error signal to be generated which changes the wheel speed in the direction causing the pitch error to decrease. The wheel control element also generates signals to fire thrusters, causing excess wheel momentum to be unloaded.
	Thruster Control The Thruster Control element implements the roll/yaw axis control law. The roll/yaw error input operates through the control transfer function and causes thruster firings oriented toward removing the roll/yaw error.
	Command Logic Processing This element accepts decoded commands for the AVCS from the S-band Command Processing function and performs operations on the commands based on a pre-set logic configuration to generate conditional command and logic configurations for use by other AVCS functional elements. The earth sensor processing, wheel control, thruster control, and command logic processing functional elements are implemented in the CEA.
	Power Switching This element switches regulated power from the spacecraft equipment converter to the various AVCS user equipment. ON/OFF and redundancy control is included. The wheel driving, valve driving, and power switching functional elements are implemented in the AEA.
	Wheel Driving This element uses the wheel control output to drive the reaction wheel at the correct speed such that the spacecraft rotates about the pitch axis once for every revolution around the earth. The wheel drive element also senses the wheel speed and supplies this value to the wheel control element so that momentum dumping requirements can be assessed.
	Valve Driving This functional element converts the thruster firing signals into valve solenoid currents so that the thrusters will fire. Provision for specific thruster selection and enabling to prevent undesired firings is included.

Figure 3.4-1. Failure Mode Data Sheets for Functional Upset of AVCS (Continued)

Wheel Control and Thruster Control

Transient upset recovery times in the analog circuits of these control law elements will be very short compared with the X- to x-second sensor processing holding register upset times. Therefore these transient response times will not significantly affect pointing error. However, both of these elements contain timing circuits and one-shots which may be triggered and/or scrambled. Transient upset of these circuits will not contribute to spacecraft pointing error, but may only cause a small increase in reaction control gas usage for a short time (less than X hour).

Command Logic Processing and Power Switching

These functional elements provide logic processing for decoded commands which set AVCS mode, status and redundancy configuration. No transient response which could cause change of mode or configuration is acceptable.

Wheel Driving and Valve Driving

Transients in the wheel driving function will have minimum effect on the wheel speed; the wheel motor time constant is too long to respond to the relatively short circuit upset times. The only significant failure mode in the wheel driving element is a possible extraneous tachometer pulse output to the wheel control element. Likewise, the time constants associated with valve solenoids are too long to respond to short-term transients in the valve drive circuits. The valve driving element could cause extraneous valve firing only through a combination of failures: undesired enabling of one or more valve drivers; mode change allowing selection of one or more valve drivers; and scrambling of the correct combination of precession, ΔV, or backup keydown registers, initiating firing of one or more of the unintentionally selected and enabled thrusters. This failure mode must be prevented since it might cause loss of earth pointing accuracy.

Wheel Control and Thruster Control

Transients shall not cause signals to be issued to the Auxiliary Electronics Assembly (AEA) so as to cause any thrusters to fire or the reaction wheel speed or direction to change so that the requirements of SS7-20 are not met.

Command Logic and Power Switching

Transients whall not cause mode changes to occur in the CEA while in the normal mode, so as to change

a) the routing of control signals in the CEA

b) gains, time constants, or other parameters outside the limits.

Transients in the AEA shall not, while in the normal mode, cause any change in mode, redundancy, configuration, or operational status.

Wheel Driving and Valve Driving

Transients in the AEA shall not, while in the normal mode, cause any change in mode, redundancy configuration or operational status, including

a) the enabling of thrusters not a part of the normal mode

b) the disabling of thrusters previously enabled for the normal mode.

Transients shall not cause any thrusters to fire or not to fire, or the reaction wheel speed of direction to change such that the requirements are not met.

Assembly (SSA). Table 3.5-1 summarizes the critical components for either thermomechanical or total dose degradation in each subassembly of the AVCS.

Preliminary Assessment Approach for Nonelectronic Components

The survivability verification done on FLTSATCOM has indicated the critical nonelectronic components of the AVCS which are susceptible to radiation effects. The assessment would begin with a functional analysis to indicate what performance criteria are required for these critical components to ensure no loss or degradation of satellite functions. Next, one must determine at what environment these criteria are no longer satisfied, i.e. determine the component failure environment. For those materials susceptible to thermomechanical effects the melting and sublimation energy must first be identified. The fluence to melt or sublime the material could then be estimated under the assumption that the incident blackbody temperature maximized the energy deposition in the material. Similarly, data must be accumulated to identify the total dose required to damage those materials susceptible to ionization damage. This total dose value can then be converted to an equivalent fluence failure. If we assume uncorrelated failure of components, it is possible to identify the subsystem fluence-to-fail with that of the softest critical component. It is likely that the materials will have much higher failure fluences than the electronic components and therefore will require no detailed analysis.

Table 3.5-1. AVCS Critical Nonelectronic Components for Radiation Damage

Subassembly	Critical Components	Damaging Effect
RWA	none	
SADA	slip ring assembly	thermal effects
ESA	germanium lens	thermomechanical
SSA	thermal control materials	thermomechanical
	Sylgard-182	total dose degradation
	vacuum deposited nickel	thermomechanical

REFERENCES

1. FLTSATCOM Survivability Critical Design Review Pacakge, 15 July 1974, Volumes I, II, III and IV, TRW No. 24200-240-005-01, Sequence Nos. A044, A056

2. Spacecraft Hardening Design Guidelines Handbook, prepared by Vulnerability and Hardness Laboratory, TRW Systems Group, December 1974.

3. A.R. Hunt, M.L. Van Blaricum, R.E. Wengler, "Satellite Nuclear Survivability Assessment Methodology (NHEP-S) Program," CR78-575, Effects Technology, Inc., 30 November 1978.

4. D.M. Clement and R.A. Lowell, "The Hardening of Satellite Cables to X-Rays," Trans. Nucl. Sci., NS-25, 1391 (1978).

5. D.M. Clement, C.E. Wuller and E.P. Chivington, "Multiconductor Cable Response in X-Ray Environments," IEEE Trans. Nucl. Sci. NS-23, 1946 (1976).

6. D.R. Alexander, et al, "Electromagnetic Susceptibility of Semiconductor Components," AFWL-TR-74-280, September 1975.

7. "Flash X-ray Test Report, FLTSATCOM Attitude and Velocity Control Subsystem," 28 September 1977, TRW No. 24200-240-074-01.

8. D.M. Clement, A.R. Carlson, and L.C. Nielsen, "The Development of SGEMP Specifications," IEEE-NS-26 (1979) (to be published).

9. FLTSATCOM Electrical Schematic Data Book, Volume I.

10. Trapped Radiation Handbook.

11. T.A. Dellin and C.J. MacCallum, "A Handbook of Photo-Compton Current Data," Sandia, SCL-RR-720086, December 1972.

12. N.J. Carron and C.L. Longmire, "Scaling Behavior of the Time-Dependent SGEMP Boundary Layer," IEEE Trans. Nucl. Sci., Vol. NS-25, No. 6, December 1978.

13. E. Vance, "Coupling to Cables," SRI, December 1974, p. 11-110.

14. G. Sower, "Coupling into Cables used on the Diablo Hawk SGEMP Experiment," DH SGEMP Memo No. 44, December 1978.

15. Wire Length Table.

16. FLTSATCOM Electrical Schematic Data Book, Vol. I.

17. FLTSATCOM System Interface Document.

18. W. Feller, Introduction to Probability Theory and its Applications, Vol. 1 (New York:Wiley, 1968).

19. C.Eisenhart, et al, Techniques of Statistical Analysis (New York:McGraw-Hill, 1975).

DISTRIBUTION LIST

DEPARTMENT OF DEFENSE

Assistant to the Secretary of Defense
Atomic Energy
ATTN: Executive Assistant

Defense Intelligence Agency
ATTN: DB-4C

Defense Nuclear Agency
2 cy ATTN: RAEV
4 cy ATTN: TITL

Defense Technical Information Center
12 cy ATTN: DD

Field Command
Defense Nuclear Agency
ATTN: FCPR
ATTN: FCLMC

Field Command
Defense Nuclear Agency
Livermore Division
ATTN: FCPRL

Interservice Nuclear Weapons School
ATTN: TTV

Joint Chiefs of Staff
ATTN: J-5 Nuclear Division
ATTN: C3S Evaluation Office

Joint Strat. Tgt. Planning Staff
ATTN: JLTW-2
ATTN: JLA

National Communications System
ATTN: NCS-TS

Undersecretary of Defense for Rsch. & Engrg.
ATTN: Strategic & Space Systems (OS)

DEPARTMENT OF THE ARMY

BMD Advanced Technology Center
Department of the Army
ATTN: ATC-O

BMD Systems Command
Department of the Army
ATTN: BDMSC-H

Deputy Chief of Staff for Rsch., Dev., & Acq.
Department of the Army
ATTN: DAMA-CSS-N

Electronics Tech. & Devices Lab.
U.S. Army Electronics R&D Command
ATTN: DRSEL

Harry Diamond Laboratories
Department of the Army
ATTN: DELHD-N-RBC, R. Gilbert
ATTN: DELHD-I-TL

DEPARTMENT OF THE ARMY

U.S. Army Communications Sys. Agency
ATTN: CCM-AD-LB

U.S. Army Foreign Science & Tech. Ctr.
ATTN: DRXST-IS-1

U.S. Army Missile R&D Command
ATTN: RSIC

DEPARTMENT OF THE NAVY

Naval Research Laboratory
ATTN: Code 6701
ATTN: Code 7550, J. Davis
ATTN: Code 6707, K. Whitney

Naval Surface Weapons Center
ATTN: Code F31

Strategic Systems Project Office
Department of the Navy
ATTN: NSP

DEPARTMENT OF THE AIR FORCE

Air Force Geophysics Laboratory
ATTN: PH, C. Pike

Air Force Weapons Laboratory
Air Force Systems Command
ATTN: SUL
ATTN: NT
ATTN: NXS
2 cy ATTN: DYC

Ballistic Missile Office
Air Force Systems Command
ATTN: MNRTE
ATTN: MNNG
ATTN: MNNH

Deputy Chief of Staff
Research, Development, & Acq.
Department of the Air Force
ATTN: AFRDQSM

Headquarters Space Division
Air Force Systems Command
ATTN: SKF

Rome Air Development Center
Air Force Systems Command
ATTN: ESR, E. Burke

Strategic Air Command
Department of the Air Force
ATTN: NRI-STINFO Library
ATTN: XPFS

DEPARTMENT OF ENERGY CONTRACTORS

Lawrence Livermore National Laboratory
ATTN: Tech. Info. Dept. Library

DEPARTMENT OF ENERGY CONTRACTORS (Continued)

Los Alamos National Scientific Laboratory
ATTN: MS 364

Sandia National Laboratories
Livermore Laboratory
ATTN: T. Dellin

Sandia National Laboratories
ATTN: 3141

OTHER GOVERNMENT AGENCY

NASA
ATTN: N. Stevens
ATTN: C. Purvis
ATTN: Library

DEPARTMENT OF DEFENSE CONTRACTORS

Aerospace Corp.
ATTN: V. Josephson
ATTN: J. Reinheimer
ATTN: Library

AVCO Research & Systems Group
ATTN: Library A830

Boeing Co.
ATTN: P. Geren

Computer Sciences Corp.
ATTN: A. Schiff

Dikewood Industries, Inc.
ATTN: Technical Library

Dikewood Industries, Inc.
ATTN: K. Lee

EG&G Washington Analytical Services Center, Inc.
ATTN: Library

Eugene P. Deplomb
ATTN: E. Deplomb

Ford Aerospace & Communications Corp.
ATTN: A. Lewis
ATTN: Technical Library

General Electric Co.
ATTN: J. Peden

General Electric Company—TEMPO
ATTN: DASIAC
ATTN: W. McNamara

Hughes Aircraft Co.
ATTN: Technical Library

Hughes Aircraft Co.
ATTN: E. Smith
ATTN: W. Scott
ATTN: A. Narevsky

DEPARTMENT OF DEFENSE CONTRACTORS (Continued)

Institute for Defense Analyses
ATTN: Classified Library

IRT Corp.
ATTN: Library
ATTN: D. Swift
ATTN: N. Rudie

JAYCOR
ATTN: E. Wenaas
ATTN: Library

JAYCOR
ATTN: R. Sullivan

Johns Hopkins University
ATTN: P. Partridge

Kaman Sciences Corp.
ATTN: W. Rich
ATTN: Library
ATTN: J. Lubell

Lockheed Missiles & Space Co., Inc.
ATTN: Dept. 85-85

McDonnell Douglas Corp.
ATTN: S. Schneider

Mission Research Corp.
ATTN: C. Longmire
ATTN: R. Stettner

Mission Research Corporation—San Diego
ATTN: V. Van Lint
ATTN: Library

R & D Associates
ATTN: C. MacDonald
ATTN: Tech. Info. Center
ATTN: L. Schlessinger
ATTN: P. Haas

Rockwell International Corp.
ATTN: Library

Science Applications, Inc.
ATTN: W. Chadsey

Spire Corp.
ATTN: R. Little

SRI International
ATTN: Library

Systems, Science & Software, Inc.
ATTN: A. Wilson
ATTN: Library

TRW Defense & Space Systems Group
ATTN: E. Chivington
ATTN: Tech. Info. Center